The RECG1 DNA Translocase Is a Key Factor in Recombination Surveillance, Repair, and Segregation of the Mitochondrial DNA in Arabidopsis

Clémentine Wallet, Monique Le Ret, Marc Bergdoll, Marc Bichara, Andre Dietrich, Jose-Manuel Gualberto

The Plant Cell, Vol. 27: 2907–2925, October 2015, www.plantcell.org

The RECG1 DNA Translocase Is a Key Factor in Recombination Surveillance, Repair, and Segregation of the Mitochondrial DNA in Arabidopsis[OPEN]

Clémentine Wallet,[a] Monique Le Ret,[a] Marc Bergdoll,[a] Marc Bichara,[b] André Dietrich,[a] and José M. Gualberto[a,1]

[a] Institut de Biologie Moléculaire des Plantes, CNRS UPR2357, Université de Strasbourg, 67084 Strasbourg, France
[b] CNRS UMR7242, IREBS, Université de Strasbourg, 67412 Illkirch, France

ORCID IDs: 0000-0002-2388-4510 (C.W.); 0000-0002-7296-2618 (J.M.G.)

The mitochondria of flowering plants have considerably larger and more complex genomes than the mitochondria of animals or fungi, mostly due to recombination activities that modulate their genomic structures. These activities most probably participate in the repair of mitochondrial DNA (mtDNA) lesions by recombination-dependent processes. Rare ectopic recombination across short repeats generates new genomic configurations that contribute to mtDNA heteroplasmy, which drives rapid evolution of the sequence organization of plant mtDNAs. We found that *Arabidopsis thaliana* RECG1, an ortholog of the bacterial RecG translocase, is an organellar protein with multiple roles in mtDNA maintenance. RECG1 targets to mitochondria and plastids and can complement a bacterial *recG* mutant that shows defects in repair and replication control. Characterization of Arabidopsis *recG1* mutants showed that RECG1 is required for recombination-dependent repair and for suppression of ectopic recombination in mitochondria, most likely because of its role in recovery of stalled replication forks. The analysis of alternative mitotypes present in a *recG1* line and of their segregation following backcross allowed us to build a model to explain how a new stable mtDNA configuration, compatible with normal plant development, can be generated by stoichiometric shift.

INTRODUCTION

Vascular plants have large mitochondrial genomes, varying from a few hundred kilobases to several megabases in size (Sloan et al., 2012) and are mostly constituted by noncoding sequences. The actual structure of these large genomes remains unclear. Although mapping and sequencing data generally produce large circular chromosomes comprising all the genetic information of mitochondria, physical observation of the mitochondrial DNA (mtDNA) using electrophoretic and microscopic approaches revealed a complex and fragmented distribution into heterogeneous populations of circular, linear, and multibranched double- and single-stranded molecules that apparently exist in dynamic equilibrium (Oldenburg and Bendich, 1996; Backert et al., 1997; Backert and Börner, 2000). Multichromosomal mitochondrial genomes have also been found in several species of flowering plants (Alverson et al., 2011; Sloan et al., 2012). Moreover, the structure of plant mitochondrial genomes evolves rapidly, driven by rearrangements that result from high rates of recombination. This rapid evolution of the mtDNA is manifest not just interspecies, but also intraspecies, and significantly different mtDNA structures can be found in different plant accessions (Allen et al., 2007; Arrieta-Montiel et al., 2009). On the contrary, gene sequences evolve very slowly in most species, apart from a few significant exceptions (Mower et al., 2007).

Our understanding of the processes that control the maintenance, replication, inheritance, and evolution of such complex and fragmented genomes remains limited. It is possible that replication of the plant mtDNA initiates by recombination-mediated processes, as in the yeast *Candida albicans* (Gerhold et al., 2010). Branched, linear, and sigma-like forms of the plant mtDNA that have been observed would be intermediates of rolling circle and/or recombination-dependent replication mechanisms, referring to the model of phage T4 (Backert and Börner, 2000). However, recombination-dependent replication does not explain how stoichiometric replication and inheritance of the fragmented mitochondrial genome is achieved. Whether there are replication checkpoints has not been documented, and it is not known whether replication of the two mtDNA strands is coupled or independent. The former is possible because the organellar replicative helicase has intrinsic DNA primase activity (Diray-Arce et al., 2013).

As to the shuffling of mtDNA sequences, it is promoted by the numerous repeated sequences present in plant mitochondrial genomes and involves (1) frequent homologous recombination (HR) via large repeated sequences, (2) ectopic recombination involving intermediate-size repeats (IRs), or (3) illegitimate recombination involving sequence microhomologies (Maréchal and Brisson, 2010; Gualberto et al., 2014). These recombination activities contribute to the intrinsic heteroplasmic state of plant mitochondrial genomes, in which alternative mitotypes coexist with the predominant mtDNA at substoichiometric levels (Small et al., 1989; Kmiec et al., 2006). In some conditions, one of the minor mitotypes can become predominant, by a stoichiometry shift of the relative copy numbers. This process has been described in many different species (Small et al.,

[1] Address correspondence to jose.gualberto@ibmp-cnrs.unistra.fr.
The author responsible for distribution of materials integral to the findings presented in this article in accordance with the policy described in the Instructions for Authors (www.plantcell.org) is: José M. Gualberto (jose.gualberto@ibmp-cnrs.unistra.fr).
[OPEN] Articles can be viewed online without a subscription.
www.plantcell.org/cgi/doi/10.1105/tpc.15.00680

1989; Kanazawa et al., 1994; Chen et al., 2011) and cybrids (Sakai and Imamura, 1992; Bellaoui et al., 1998) and can occur in the time frame of just a few generations. It is also at the origin of cytoplasmic male sterile varieties of agronomic interest and of corresponding fertile revertants (Janska et al., 1998; Allen et al., 2007; Feng et al., 2009; Matera et al., 2011). Thus, rapid evolution of the mtDNA involves recombination processes that promote mtDNA heteroplasmy and sorting of the alternative mitotypes by stoichiometric shifting.

The mechanisms of mitochondrial recombination that promote mtDNA variability have only started to be unraveled. The "raison d'être" of these recombination pathways apparently is the repair of mtDNA lesions (Davila et al., 2011; Christensen, 2013). The response to genotoxic stress that comes out with increased HR between IRs is controlled by genes involved in repair, several of which have been identified (*RECA HOMOLOG3* [*RECA3*], *WHIRLY2* [*WHY2*], *ORGANELLAR DNA BINDING PROTEIN1* [*ODB1*], and *DNA POLYMERASE 1B* [*POL1B*]). In the corresponding mutants, there is reduced repair by homologous recombination and there might be increased illegitimate recombination involving sequence microhomologies (Cappadocia et al., 2010; Parent et al., 2011; Janicka et al., 2012; Miller-Messmer et al., 2012). These illegitimate recombination events are possibly responsible for U-turn genomic inversions that accumulate in plant organelles and also in human mitochondria (Zampini et al., 2015).

Because of the deleterious nature of the rearrangements that can be created by recombination processes, these are under tight control, and undesired recombination activities are normally suppressed. Restriction of ectopic and illegitimate mtDNA recombination might occur during replication, while rescuing stalled replication forks, or at the postreplicative level, through dissociation of D-loops formed by strand invasion at ectopic DNA locations. The recombination surveillance pathways are disrupted in the mutants of several genes, such as the mutants of *MUTS HOMOLOG1* (*MSH1*), *ORGANELLAR SINGLE-STRANDED DNA BINDING PROTEIN1* (*OSB1*), *RECA2*, and *RECA3* (Zaegel et al., 2006; Arrieta-Montiel et al., 2009; Miller-Messmer et al., 2012). In these mutants, there are increased rates of ectopic recombination involving IRs, which in later mutant generations can result in stoichiometric shifting (Zaegel et al., 2006; Davila et al., 2011). The study of these mutants advanced our understanding of the factors that can promote mtDNA evolution by stoichiometric shifting, but the examples that have been described involved multiple events of recombination, difficult to follow individually, and the dynamics of the shifting process leading from one predominant mtDNA structure to another could not be understood.

For a deeper understanding of these processes, we searched for specific DNA helicases that could play essential roles in mtDNA maintenance, in particular in the orientation toward error-free recombination and replication processes. We identified the *Arabidopsis thaliana* RECG1 helicase, an ortholog of bacterial RecG. We show that RECG1 has multiple roles in mtDNA repair by recombination and in the suppression of ectopic recombination events. Remarkably, whereas mutations of so far identified mitochondrial recombination factors triggered multiple and complex events of recombination, a *recG1* mutation generated only two alternative configurations of the mitochondrial genome differing in a single locus. This convenient system allowed us to study the dynamics of their segregation in the following generations, a process influenced by RECG1, and to build a model for the transition to a new stable mtDNA structure compatible with normal plant development by stoichiometric shift.

RESULTS

We screened the *Arabidopsis* genome for genes coding for candidate DNA helicases potentially involved in mtDNA recombination. Because the recombination machineries of plant organelles are partially inherited from their symbiotic ancestors, we have in particular searched for orthologs of bacterial DNA helicases with known functions in recombination processes. Our scrutiny mainly retrieved a homolog of bacterial RecG. Other prokaryotic-type DNA helicases either are not encoded in plant genomes (i.e., RuvAB), have no putative organellar targeting sequences, or have been studied already, with no hint of possible functions in organellar processes (i.e., RecQ-like proteins)(Knoll and Puchta, 2011). In bacteria, RecG is a DNA translocase that can perform multiple functions, including Holliday junction (HJ) resolution, rescuing of stalled replication forks, modulation of RecA-promoted strand exchange, and suppression of pathological DNA replication (Vincent et al., 1996; McGlynn and Lloyd, 2002; Rudolph et al., 2010, 2013). The RecG homolog is encoded in all sequenced plant genomes, including vascular plants, mosses, and algae (Supplemental Figure 1). We named the Arabidopsis RecG RECG1.

RECG1 Is Conserved in All Plant Species and Is Targeted to Both Mitochondria and Chloroplasts

Phylogenetic analysis shows that plant RECG1s branch together with cyanobacterial RecG proteins, suggesting that the plant gene was inherited from the symbiotic ancestor of the chloroplast (Figures 1A; Supplemental Figure 1). A three-dimensional model of the Arabidopsis RECG1 could be generated (Figure 1B) on the basis of the known RecG structure of *Thermatoga maritima* that has been solved in complex with a replication fork analog (Singleton et al., 2001). The RecG structure comprises three domains, two of which form the core helicase motor. The large third domain contains a Greek key fold that acts as a "wedge," directing the template strand toward the core motor and steering the second strands of the side arms to facilitate their annealing. This mechanism can explain HJ branch migration, regression of replication forks into HJ, and unwinding of D-loops and R-loops, i.e., all functions that have been proposed for RecG (McGlynn and Lloyd, 2002; Briggs et al., 2004) and for its phage T4 functional homolog UvsW (Carles-Kinch et al., 1997; Dudas and Kreuzer, 2001; Manosas et al., 2013). All major domains of the plant RECG1 model perfectly match the bacterial structure (Figure 1B), supporting the assumption that RECG1 has the same activities as the bacterial enzyme and potentially has similar functions. Notably, all plant proteins share three additional short extensions that are not found in bacterial sequences (Figure 1A; Supplemental Figure 2) and that could not be accommodated into the model. These extensions (of 20, 15, and 19 amino acids, respectively, in Arabidopsis RECG1) might confer specific characteristics to plant RECG1s.

All plant sequences present N-terminal extensions that could correspond to organellar targeting peptides (Supplemental Figure 2), and the Arabidopsis RECG1 is predicted to be targeted to

organelles (http://suba.plantenergy.uwa.edu.au). This assumption was tested by expression of a construct encoding the N terminus of RECG1 fused to eGFP. Subcellular localization of the fusion protein was analyzed both in transfected *Nicotiana benthamiana* leaf cells and in stable Arabidopsis transformants, and in both systems the protein was found in chloroplasts and in mitochondria (Figure 1C), implying that RECG1 is an additional example of a dually targeted organellar protein. Recently, the *Physcomitrella patens* ortholog of Arabidopsis RECG1 was described and shown as well to be targeted to both mitochondria and chloroplasts (Odahara et al., 2015).

Expression of *RECG1* during plant development was studied in Arabidopsis lines stably transformed with the β-glucuronidase gene under the control of the *RECG1* promoter. The consensus observation from several independent transformants was that the *RECG1* promoter was active at all developmental stages and in most tissues, including shoots of young plants, root tips, and secondary root primordia. High expression was observed in the vascular tissues of leaves and roots (Figure 1D). In mature flowers, β-glucuronidase was present in sepals and in stamen filaments, but not in pollen, ovules, or developing seeds.

RECG1 Partially Complements Bacterial RecG

The ability of plant RECG1 to complement *Escherichia coli* RecG in repair of UV-C-induced DNA lesions was tested, as described in Methods. UV-C promotes formation of pyrimidine dimers that block the replication fork and induce repair mechanisms in which RecG is implicated (Meddows et al., 2004). After UV-C irradiation, the Δ*recG* strain presented a 30-fold decrease in survival, as described before (Lloyd, 1991). Expression of the plant RECG1 significantly increased the survival rate of Δ*recG* upon UV exposure (Figure 2A). When bacteria were irradiated with up to 20 J/m^2 of UV-C, the survival of complemented mutant cells increased by a factor of 15-fold compared with the noncomplemented mutant, reaching half of the survival rate of wild-type bacteria. We also tested

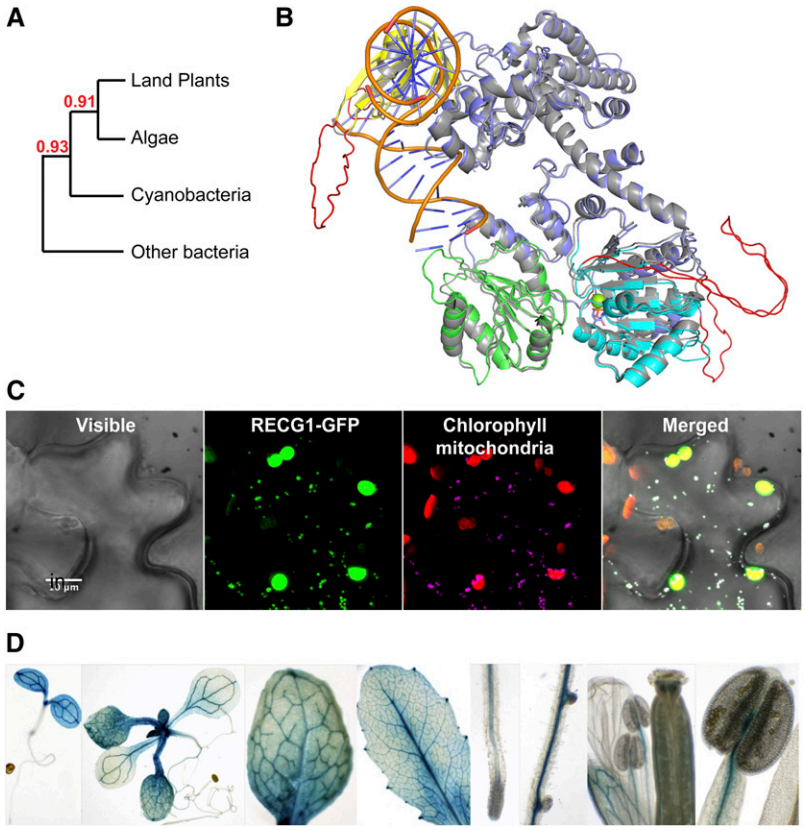

Figure 1. A RecG Protein Is Present in the Organelles of Plants.

(A) Detail of the RecG phylogenetic tree supporting that plant RecGs derive from a cyanobacterial ancestor. Bootstrap values are indicated.
(B) Model of the Arabidopsis RECG1 protein superposed on the known structure of *T. maritima* RecG (in gray) bound to a DNA substrate mimicking a stalled replication fork (Singleton et al., 2001). The large N-terminal domain is in purple, with the wedge domain in yellow. The two helicase domains are in green and light blue, with complexed ADP and Mg^{2+} (green ball). The three sequences specific to plant RecGs (see alignment in Supplemental Figure 2) could not be modeled and are shown in red.
(C) Transient expression of the RECG1-GFP construction in *N. benthamiana* leaf epidermal cells showing dual targeting of RECG1. Chloroplasts and mitochondria are identified by the fluorescence of the chlorophyll and by coexpression of a CoxIV-dsRED construct, respectively.
(D) Widespread expression of *RECG1* in Arabidopsis, according to promoter-GUS fusion at different developmental stages. From left to right, 3-d-old and 7-d-old seedlings, rosette and cauline leaves, roots, flowers, and anthers.

whether the Arabidopsis RECG1 could complement a deficiency in *RuvAB* because both RecG and RuvAB are translocases that drive branch migration and have been described as either partially redundant or complementary in the resolution of HJ (Zhang et al., 2010; Mawer and Leach, 2014). In contrast to Δ*recG*, the Δ*ruvA* mutation could not be rescued by RECG1 (Figure 2A). Thus, despite the absence of RuvAB in plant organelles, RECG1 has not acquired RuvAB-like functions during evolution and apparently has similar specificity in DNA repair as bacterial RecG.

In addition to its function in DNA repair, bacterial RecG has recently been assigned as a guardian of the bacterial genome that prevents pathological re-initiation of DNA replication (Rudolph et al., 2013). In *E. coli*, genome replication initiates bidirectionally at the *OriC* region and proceeds around the circular genome in both directions. Therefore, in wild-type exponentially growing bacteria, a maximum in copy number is found for the sequences around the *OriC* region and a minimum for the region between the termination sequences *TerA* and *TerB* (Figure 2B). In the absence of RecG, replication can reinitiate where forks collide by a process that depends on recombination functions (Rudolph et al., 2013). We tested the ability of RECG1 to prevent replication reinitiation by quantifying the relative copy number of the *YdcR* gene located equidistantly between *TerA* and *TerB*, as described in Methods. It was found that in Δ*recG* there was indeed a significant increase in *YdcR* copy number compared with the wild type (Figure 2B), indicating replication restart in the termination zone and confirming published results (Rudolph et al., 2013). When RECG1 was expressed in the Δ*recG* mutant, this effect was reduced, although not abolished, showing that RECG1 can partially replace bacterial *recG* in the suppression of uncontrolled replication reinitiation. This result also suggests that RECG1 might be necessary for stoichiometric replication of the plant organellar genomes.

Finally, we tested whether RECG1, like RecG, is able to dissociate R-loops, and as a consequence inhibit the replication of plasmids containing ColE1 replicons (Vincent et al., 1996). Replication of these plasmids is primed by a short RNA expressed from the replication origin (Dasgupta et al., 1987). The wild-type, Δ*recG*, and Δ*recG RECG1*+ strains were transformed with ColE1-based plasmids (pBAD/Thio or pUC18) whose relative copy numbers in exponentially growing cultures were compared with the copy numbers in saturated precultures. In nonselective growth conditions, a 3-fold lower copy number of the plasmids was retained in the complemented strain compared with the Δ*recG* strain, comparable to the relative copy numbers found in the wild-type strain. This result indicated that expression of RECG1 inhibited the replication of ColE1-based replicons (Figure 2C).

Arabidopsis Plants Deficient in RECG1 Have Reduced Recombination-Dependent mtDNA Repair

From a search of the available T-DNA insertion mutant collections, only two confirmed *recG1* lines were obtained (Figure 3A), one in accession Col-0 containing an insertion in the 5′-untranslated region (UTR) of *RECG1* (*recG1-1*) and a second one in accession Wassilewskija (Ws) containing a T-DNA insertion in the last but one exon (*recG1-2*). The insertion in *recG1-2* results in the loss of the last 126 codons, part of which encode a highly conserved helical hairpin motif essential for helicase activity (Mahdi et al., 2003). Quantification by RT-qPCR showed that both lines have a significant decrease in *RECG1* transcript, of about 5-fold (Figure 3B). Immunoblot analysis with a specific antibody against RECG1 showed that *recG1-1* is a hypomorphic mutant that has a significant reduction in RECG1 protein, while *recG1-2* is a knockout in which the protein is no longer detected (Figure 3C). Under normal growth conditions, both *recG1-1* and *recG1-2* plants were indistinguishable from wild-type plants.

In bacteria, RecG is required for recombination-dependent DNA repair (Lloyd and Buckman, 1991), and the above assays suggest that RECG1 can complement this function. To test whether RECG1 plays a similar role in plant mitochondria, the growth of *recG1-1* and *recG1-2* seedlings was examined under genotoxic stress, more specifically under exposure to ciprofloxacin (CIP). CIP is an inhibitor of gyrase, an enzyme that in plants is active in both mitochondria and chloroplasts but not in the nucleus (Wall et al., 2004). Gyrase inhibition by CIP promotes double-strand breaks (DSBs), and mutants for genes involved in organellar HR-dependent repair are more sensitive to CIP than the wild type (Cappadocia et al., 2010; Rowan et al., 2010; Parent et al., 2011; Janicka et al., 2012; Miller-Messmer et al., 2012; Lepage et al., 2013). Seedlings of *recG1-1*, *recG1-2*, and of the corresponding wild-type lines were grown in the presence of CIP, and the ability to develop normal first true leaves was scored, as previously described (Parent et al., 2011; Miller-Messmer et al., 2012). The Col-0 and Ws wild-type accessions were differentially sensitive to CIP, with Ws slightly more sensitive than Col-0: At 0.75 μM CIP, ~20% of the Col-0 plants still developed first leaves while virtually none of the Ws seedlings did (Figure 4A). Regarding the mutant lines, both *recG1-1* and *recG1-2* were slightly more sensitive than the corresponding wild-type accessions, with fewer mutant seedlings developing true first leaves (Figures 4A and 4B).

Repair by recombination of mtDNA DSBs is also correlated to the molecular phenotype of increased ectopic recombination across IR sequences. This response is reduced in several mutants impaired in HR-dependent repair (Janicka et al., 2012; Miller-Messmer et al., 2012). Therefore, the levels of ectopic recombination across mtDNA IRs were also compared between CIP-treated and untreated seedlings, for wild-type and *recG1* lines (Figures 4C and 4D). The sequence and organization of the mtDNA are known for Col-0 (accession JF729201) but not for Ws. To compare the two *recG1* mutant alleles, which have different genetic backgrounds, we first tested the mtDNA of the Ws accession for the presence of IRs that are also contained in the Col-0 mitochondrial genome. We found that few IRs previously described as involved in ectopic recombination in Col-0 mitochondria are conserved in the Ws mtDNA (Supplemental Figure 3). We analyzed the ectopic recombination involving repeats D, L, X, and EE, according to the nomenclature of the published mtDNA of Col-0. Sequence L could not be tested in *recG1-2* because it is not repeated in the mtDNA of Ws. In the two wild-type accessions, upon CIP exposure there was a significant increase in ectopic recombination involving all repeats tested, as previously described (Miller-Messmer et al., 2012). The recombination was in all cases asymmetric, with one of the crossover products preferentially increased compared with the reciprocal one (Figure 4D). The magnitude of the increase varied significantly depending on the repeat and the Arabidopsis wild-type accession: In the case of repeat X, there was only a slight increase in Ws plants of crossover product X-2/1, while the increase of the same sequence was 10-fold higher in

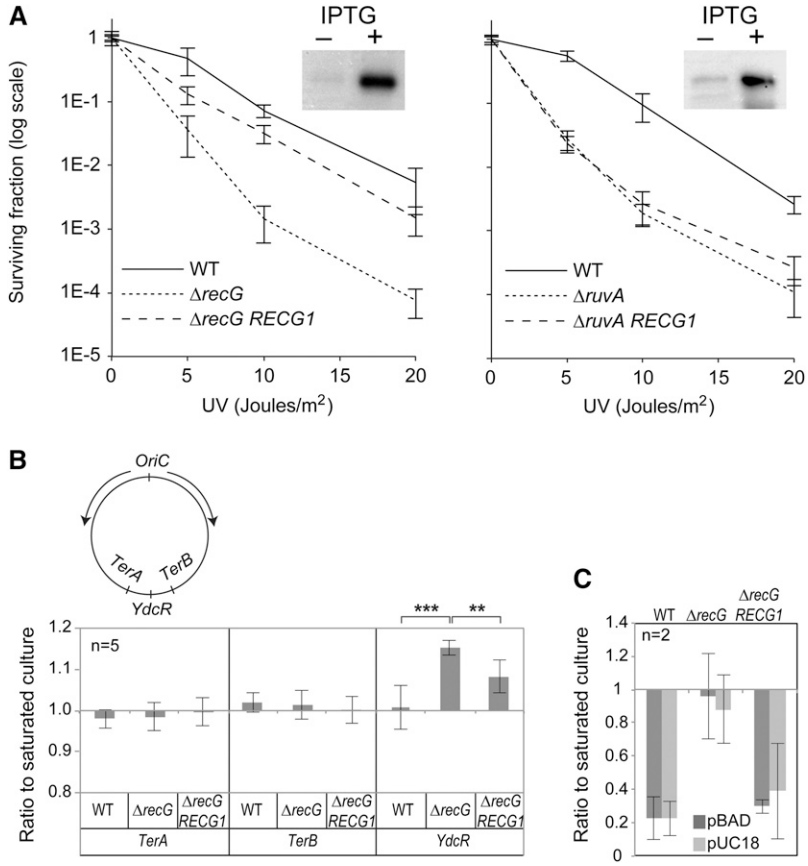

Figure 2. Arabidopsis RECG1 Partially Complements RecG Deficiency in Bacteria.

(A) Partial complementation of *E. coli* Δ*recG* but not of Δ*ruvA* in the repair of UV-C induced damage. JM103 (WT), JM103 *recG::kan* (Δ*recG*), and JM103 *ruvA::Tc* (Δ*ruvA*) transformed with the *pACYClacz* empty vector were used as control strains and compared with the ones transformed with *pACYClacz:RECG1*. Recombinant RECG1 expression was induced with IPTG prior to treatment with UV-C, as described in Methods, and controlled by immunodetection with the RECG1 antibody (on the upper right of the graphics, +/− IPTG). Results are means from two independent experiments, with three technical replicates each, and are represented on a logarithmic scale.

(B) Complementation of Δ*recG* by RECG1 in the suppression of pathologic replication reinitiation. The sequences *TerA*, *TerB*, and *YdcR* were quantified in growing cultures and the levels were compared with those in the corresponding saturated cultures. The relative positions in the *E. coli* chromosome and the divergent replication from *OriC* are shown in the scheme. Results correspond to five independent experiments ± SD. Asterisks show the statistical significance (unpaired *t* test; **P < 0.01, ***P < 0.001).

(C) Effect of RECG1 expression on the replication of plasmids (pBAD/Thio and pUC18) containing a ColE1 replication origin. Results were normalized against the bacterial chromosome (*TerA* sequence).

Col-0 plants. In the case of crossover product EE-2/1, the increase was more than 1000-fold in CIP-treated Col-0 plants, but only ~50-fold in Ws. These differences do not correlate with repeat size, but are probably related to the genomic context. But in all cases, the CIP-induced increase in crossover products was significantly lower in both mutant *recG1* lines. These results imply that reduction or loss of RECG1 expression impairs recombination-dependent repair of DSBs in the mtDNA.

We also tested whether RECG1 takes part in chloroplastic recombination-dependent repair. In contrast to the mtDNA, the chloroplast DNA (cpDNA) of Arabidopsis is not rich in IRs whose recombination can be used to monitor HR-dependent repair. We identified a single imperfect repeat (76 bp, 92% identity) amenable to qPCR analysis (a repeat that we named R2, coordinates 38705:38780 and 40929:41004 on the published cpDNA of Arabidopsis). We found that CIP-treated wild-type plants accumulated high levels of a crossover product from repeat R2, confirming that recombination involving this repeat is a good sensor of HR-dependent DSB repair in the Arabidopsis chloroplast (Figure 4E). However, *recG1* mutants displayed a similar response with no or little quantitative difference compared with the wild type, suggesting that RECG1 is not essential for chloroplastic repair of DSBs.

RECG1 Participates in the Surveillance of mtDNA Recombination

Several Arabidopsis mutants described as affected in recombination surveillance (*msh1*, *osb1*, *recA2*, and *recA3*) showed, in normal growth conditions, increased ectopic recombination of

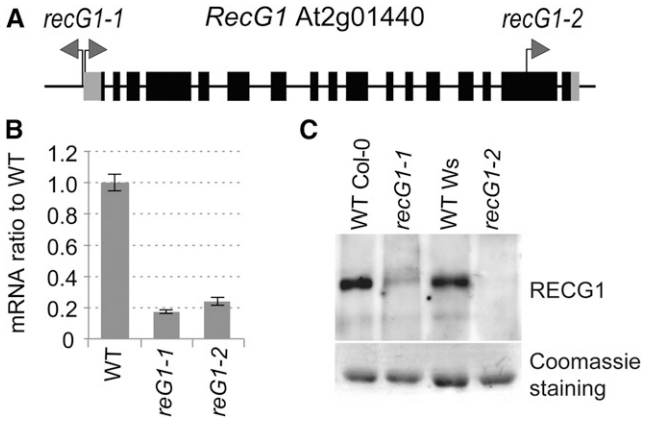

Figure 3. Arabidopsis *recG1* Lines.

(A) Schematic representation of the Arabidopsis *RECG1* gene. Coding sequences are in black and 5′- and 3′-UTRs are in gray. The position of the T-DNA insertions in the mutant lines is shown, with arrows indicating the orientation of the left border.

(B) RT-qPCR relative quantification of the *RECG1* transcript in the mutant lines.

(C) Immunodetection of RECG1 in total inflorescence extracts. Coomassie blue staining of the membrane is shown as a loading control. A protein of ~110 kD is detected in extracts from wild-type plants, in agreement with the predicted size of 108 kD. The protein is reduced in *recG1-1* and absent in *recG1-2*.

the mtDNA across IRs (Zaegel et al., 2006; Shedge et al., 2007; Miller-Messmer et al., 2012). In these mutants, without any genotoxic treatment there is already a constitutive increase in error-prone recombination activities. The *recG1* mutants were thus tested for such a molecular phenotype. The IRs D, F, X, and EE that are conserved in the mtDNA of both Col-0 and Ws (Supplemental Figure 3) were selected for qPCR analysis of the accumulation of crossover products, as previously described (Miller-Messmer et al., 2012). A significant increase in crossover products compared with wild-type levels was observed in both mutants (Figure 5A). The most important effects were in *recG1-2* KO plants, which for certain repeats showed an increase in crossover products one order of magnitude higher than in the hypomorphic *recG1-1* mutant. Recombination in *recG1* plants resulted either in equivalent accumulation of both reciprocal products (as for repeats D, F, and EE) or in asymmetrical accumulation of mainly one of the two products (as for repeat X). As the ectopic recombination induced by CIP treatment, depending on the repeats there were remarkable quantitative differences (Figure 5A). In particular, crossover products from the recombination involving repeats EE increased ~1000-fold in *recG1-2* compared with wild-type plants. To test whether loss of RECG1 also affects surveillance of recombination in the chloroplast, we monitored the ectopic recombination involving repeat R2. We found that RECG1 had little or no effect on the recombination involving this chloroplast repeat (Figure 5B). This suggests that RECG1 has no significant roles in the surveillance of recombination in the chloroplast, contrarily to its function in mitochondria.

It has been described that several mutants affected in organellar genome recombination surveillance or in repair by recombination can display visible phenotypes of reduced growth, distorted leaves, variegation, and reduced fertility, but with low penetrance or only in late mutant generations (Zaegel et al., 2006; Maréchal and Brisson, 2010; Davila et al., 2011). However, no such phenotypes were observed in homozygous *recG1* plants of generations up to T5. We screened the development of more than 100 individual T5 mutant plants from the *recG1-2* knockout line, but none showed an altered visible phenotype.

Increased Recombination in *RECG1* Knockout Plants Causes Segregation of a Small Crossover Product That Replicates Autonomously

To test the effect of increased recombination in *recG1* mutants on the relative copy number and segregation of the different mtDNA regions, the complete mtDNA was scanned by qPCR using a set of primer pairs spaced 5 to 10 kb apart (Figure 6A). The published Arabidopsis Col-0 mtDNA sequence was taken as a reference. No significant changes in the relative copy number of the different regions were detected in the *recG1-1* hypomorphic line, consistent with the partial reduction in RECG1 and the mild effect on ectopic recombination. However, in the *recG1-2* knockout, the specific amplification of an mtDNA discrete region was observed. Amplification was by a factor ranging from 4 to 8, depending on the pool of plants analyzed, and it was seen in all independent first generation homozygote plants tested. A detailed analysis showed that this stoichiometry change corresponded to the 8.0-kb region flanked by the 127-bp-long EE repeats (Figure 6B). This region contains the *ATP1* gene, coding for subunit alpha of the mitochondrial ATP synthase. The increase in copy number of this sequence resulted from the massive increase in crossover products EE-1/2 and EE-2/1 compared with the wild type (Figure 5) and was accompanied by a decrease of about 2-fold in the parental sequences EE-1/1 and EE-2/2 (Figures 5 and 6B). From this result, it was inferred that in *recG1-2*, recombination involving repeats EE produced an alternative form of the mitochondrial genome that coexists with the wild-type mtDNA. It consists in the deleted mtDNA sequence without the region between the EE repeats (EE-1/2 configuration; Figure 6D) plus an episome comprising *ATP1* (EE-2/1 configuration). Moreover, the EE-2/1 form was present at a significantly higher copy number, suggesting that once generated through recombination it is replicated autonomously and faster than the main genome.

Upon DNA gel blot analysis, an extra band that could correspond to the EE-2/1 circular episome was detected in nondigested DNA of *recG1-2*, in addition to the bulk of high molecular weight mtDNA (Figure 6C). As expected, this form was not detected with a probe hybridizing upstream of EE-1/1. Surprisingly, according to the signal intensities, the putative circular episome seemed to exist at a lower copy number than the high molecular weight mtDNA. Conversely, after restriction, the 2.7-kb *Bam*HI fragment specific of EE-2/1 was at least 4-fold more abundant than the wild-type-specific fragment of 7.7 kb according to phosphor imager quantification (Figure 6C), which was in agreement with the above qPCR results. This suggests that amplification of the recombination-generated EE-2/1 circular form produces high molecular weight DNA. It could be catenated forms of the replicating episome or tandem-repeated concatemer

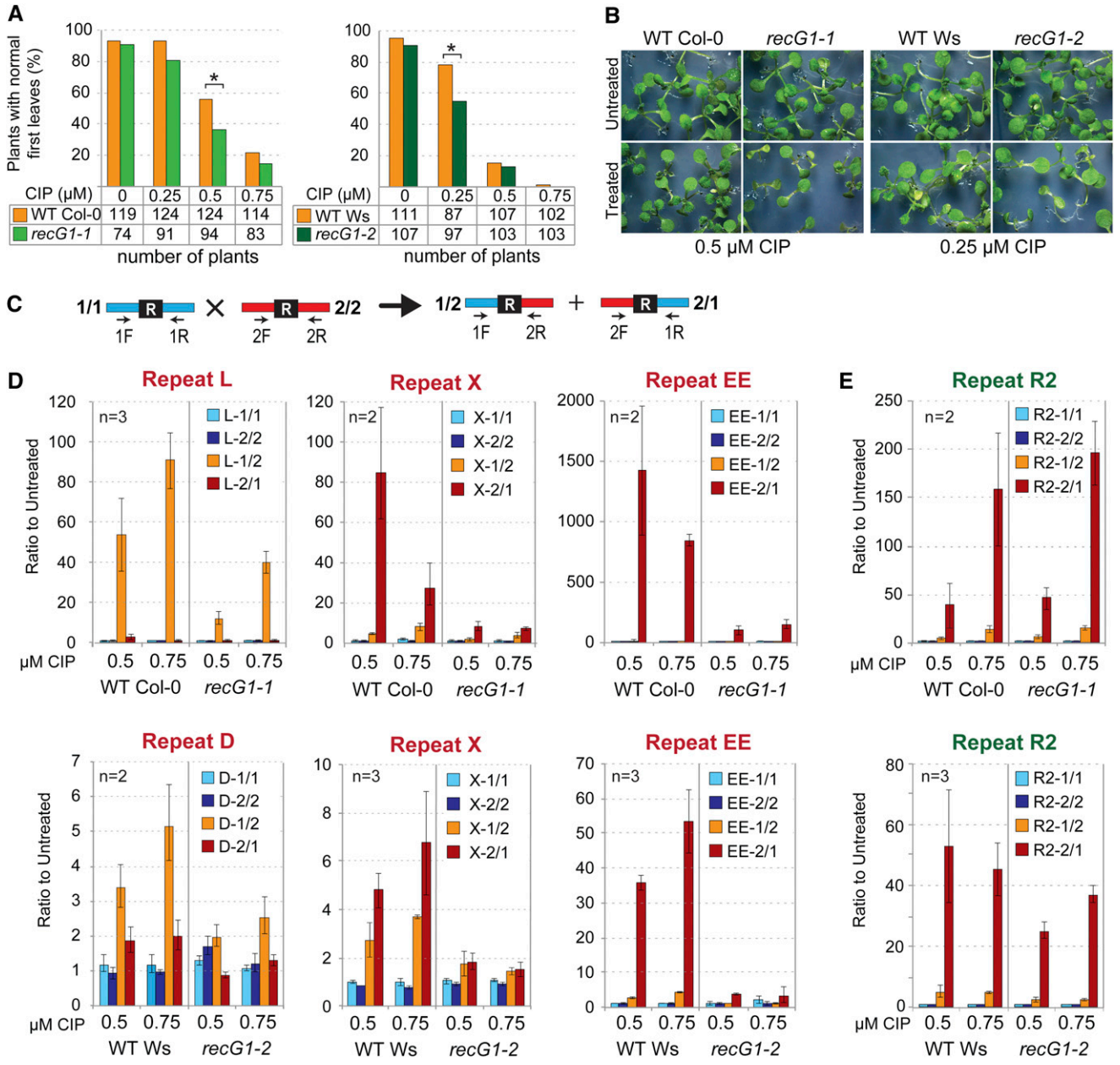

Figure 4. The *recG1* Mutants Are More Sensitive to Genotoxic Treatment and Are Deficient in HR-Dependent Repair of DSBs Induced by CIP.

(A) Percentage of plants developing normal first true leaves at the indicated concentrations of CIP. The number of plants analyzed is indicated under the graphs. Asterisks show statistical significance (unpaired *t* test; $P < 0.05$).

(B) Phenotypes of plants grown on agar plates containing the indicated concentrations of CIP. Most *recG1* plants did not develop normal first true leaves at CIP concentrations that had a mild effect on the wild type.

(C) Scheme of the qPCR relative quantification of parental sequences 1/1 and 2/2 that comprise a same repeated sequence (box R) and of the corresponding crossover products 1/2 and 2/1 using combinations of forward (F) and reverse (R) primers.

(D) Analysis of the accumulation of crossover products in CIP-treated wild-type Col-0, *recG1-1*, wild-type Ws, and *recG1-2* plants. qPCR results for repeats were normalized against the mitochondrial *COX2* and *RRN18* gene sequences. Results are the mean of two or three independent experiments, as indicated, and error bars correspond to SD values. The repair of DSBs induced by CIP in the mtDNA results in increased mobilization of IRs and concomitant accumulation of crossover products. This effect is strongly impaired in *recG1* plants.

(E) Accumulation of crossover products from chloroplast repeat R2, showing no significant effect of RECG1 in the repair of DSBs induced by CIP in the cpDNA. Results were normalized against the chloroplastic *RRN16* gene sequence.

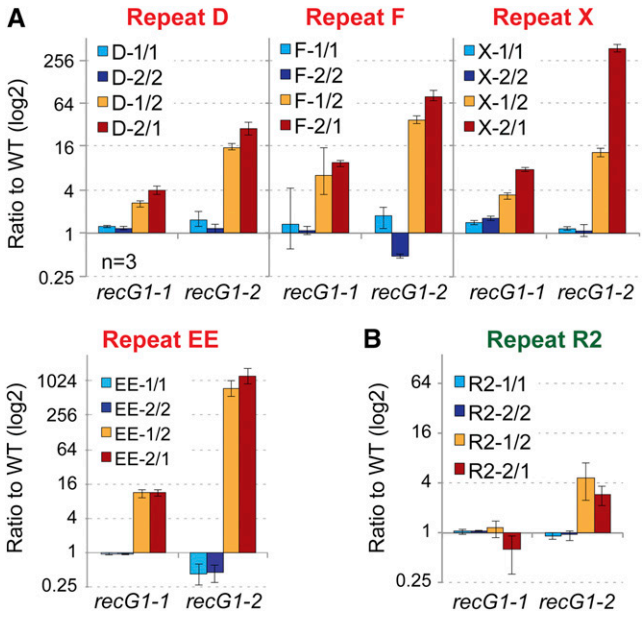

Figure 5. *recG1* Mutants Have Increased Ectopic Recombination across Mitochondrial Intermediate Size Repeats.

(A) As described in Figure 4C, quantification of the accumulation of crossover products from mitochondrial repeats D, F, X, and EE in *recG1-1* and *recG1-2* relative to the corresponding Col-0 and Ws wild-type accessions. Results are in a $\log_2$ scale.
(B) As in **(A)**, for chloroplastic repeat R2.

sequences generated by "rolling circle" replication, a process that has been proposed to occur in plant mitochondria (Backert et al., 1996). To confirm that the putative episome is indeed a circular molecule, it was digested with *Pac*I, an enzyme that cuts only once in the sequence and resolved on low percentage agarose gels (Figure 6C). *Pac*I digestion converted the molecular form migrating at an apparent size of 10 kb, which could correspond to a circular nicked molecule, into the expected linear fragment of 8 kb. Because the EE-2/1 recombination product contains *ATP1*, we checked whether its amplification results in increased expression of this gene. Indeed, a 3-fold increase in *ATP1* transcript was found in *recG1-2*, while no such increase was observed for other mtDNA gene transcripts (Figure 6E).

The cpDNA of *recG1-1* and *recG1-2* was likewise scanned for changes in sequence stoichiometry. No changes were detected between the mutants and corresponding wild-type accessions, apart from a slight general increase in cpDNA copy number (Supplemental Figure 4). Thus, loss of RECG1 does not seem to significantly affect the stoichiometric replication and segregation of the cpDNA in Arabidopsis.

RECG1 Works Synergistically with RECA3 in the Maintenance of mtDNA Stability

A comparison between the molecular effects observed in mutants of factors involved in mtDNA recombination suggests that RECG1 acts in the same pathways as the mitochondrial RecA-like protein RECA3. Both *recG1* (this work) and *recA3* (Miller-Messmer et al., 2012) mutants show increased ectopic recombination involving IRs in nonselective conditions, as well as reduced HR-dependent repair of CIP-induced mtDNA breaks. In contrast, other mutants described as involved in recombination surveillance and/or repair in plant mitochondria either are only affected in repair of induced DNA lesions (i.e., *odb1*, *why2*, and *pol1B*; Cappadocia et al., 2010; Parent et al., 2011; Janicka et al., 2012) or show only increased ectopic recombination in normal growth conditions (i.e., *osb1*; Zaegel et al., 2006). We tested the effect of the double mutation *recG1-1 recA3-2* (both mutations in the Col-0 background) on the maintenance of the Arabidopsis mtDNA. While the parental plants used for reciprocal crossing had no visible developmental phenotypes, the homozygous F2 double mutants were all affected, to different extents, by slow growth, deformed and variegated leaves, and partial or complete sterility (Figure 7A). We scanned individual plants for changes in the stoichiometry of the different mtDNA regions, as described above. All *recG1-1 recA3-2* plants tested showed substantial changes in the stoichiometry of mtDNA sequences compared with wild-type plants (Figure 7B). An increase in copy number of large regions was mainly observed that could be as high as 12-fold in some cases (e.g., plant #6). The mtDNA sequences affected and the magnitude of the changes varied from plant to plant, however, with an involvement of common specific regions. Several of the observed events of stoichiometric shift could be explained by the same process as the one involving the EE repeats in *recG1-2*: a looping out of subgenomic regions by recombination across directly oriented IRs, followed by their autonomous replication. The increase of the EE repeat regions was also observed in several plants, although it had not been seen in the hypomorphic *recG1-1* single mutant. Thus, reduction in RECG1 has a synergistic effect with the *recA3* mutation, leading to the generation by recombination of subgenomes whose replication is apparently not coordinated in these mutants.

Backcrossing Elicits Segregation of the Alternative mtDNA Forms

We have found that in *recG1-2* there is coexistence of two alternative mtDNA configurations interconvertible through a single recombination event involving the EE repeat. These are the wild-type mtDNA containing the EE-1/1-EE-2/2 region and the alternative mitotype comprising the mtDNA deprived of the EE region (EE-1/2) plus the EE-2/1 episome (Figure 6D). The simplicity of this genomic configuration makes it a convenient model to study the mechanisms and dynamics of mtDNA evolution by stoichiometric shifting and to determine how RECG1 can affect these processes. For such studies, we first analyzed the stability of the different genomic environments and their possible segregation in the wild-type and *recG1-2* populations. We found that the ratios between the main genome sequences and crossover products EE-1/2 and EE-2/1 were very well conserved among individual wild-type plants (Figure 8A), confirming the tight control that exists on mtDNA recombination.

Next, we tested whether the coexistence of the alternative mitotypes was stable in the *recG1-2* line. All first homozygous mutant plants that were tested had the molecular phenotype of increased copy number of the EE-2/1 sequence. In the progeny of one of these plants, we tested the possible segregation of the different EE configurations. More than 100 plants from generation

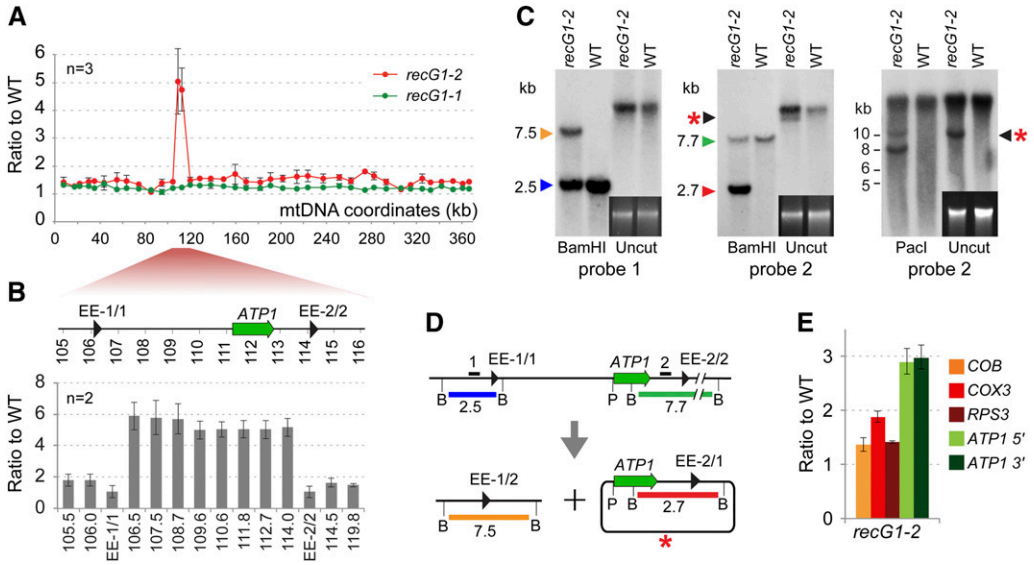

Figure 6. Recombination-Mediated Segregation of a Small Replisome Containing the *ATP1* Gene in the *recG1-2* Knockout.

(A) Scanning of the mtDNA for changes in relative copy numbers of the different mtDNA regions. Sequences spaced 5 to 10 kb apart on the mtDNA were quantified by qPCR on *recG1* mutants and corresponding wild-type accessions. Results are the mean and SD values from three biological replicates. Coordinates are those of the published Col-0 mtDNA sequence.

(B) Detailed analysis of the region amplified in *recG1-2*, using probes spaced 1 kb apart and primers that specifically amplify repeated sequences EE-1/1 and EE-2/2.

(C) DNA gel blot hybridization of wild-type and mutant DNA from inflorescences with probes external (1) and internal (2) to the amplified region. The ethidium bromide-stained uncut DNA is shown as loading control.

(D) Schematic interpretation of the results of **(C)**. *Bam*HI and *Pac*I sites are indicated and the relevant restriction fragments are color-coded. The thick lines labeled 1 and 2 indicate the sequences used as probes. Recombination involving direct repeats EE produces an alternative genome deleted of the region comprising *ATP1* and a circular sequence containing *ATP1* that is autonomously replicated and amplified in the *recG1-2* line. A red asterisk indicates the signal corresponding to the EE-2/1 episome in uncut DNA. *Pac*I digestion showed that it is a circular molecule.

(E) Increased accumulation of *ATP1* transcripts correlates with the increased gene copy number. The transcripts of several mtDNA-encoded genes including *ATP1* were quantified by RT-qPCR. Two different *ATP1* sequences from the 5′ and 3′ parts of the gene were tested.

T5 were tested by competitive PCR, but in none of these plants we found evidence for differential segregation of the alternative mitotypes. From these plants, 42 were further analyzed by qPCR, which confirmed that the ratios between the alternative EE sequences were relatively stable in the *recG1-2* background (Figure 8A). These results contrast with the data obtained for other Arabidopsis mutants affected in mtDNA recombination surveillance, including *osb1* and *msh1*, for which shifts in mtDNA structure could be observed between individuals in the mutant population, as well as segregation of plants developing specific phenotypes aggravated in late mutant generations (Zaegel et al., 2006; Shedge et al., 2007; Davila et al., 2011).

We next verified whether reintroduction of the *RECG1* allele could promote reversion to the wild-type mtDNA stoichiometry. The *recG1-2* mutant was backcrossed with wild-type Ws as pollen donor and F1 plants were analyzed. Surprisingly, among the F1 plants, ~20% displayed characteristic phenotypes of leaf distortion, variegation, slow growth, and reduced fertility (Figure 8B). These phenotypes were similar to the ones observed in the *recG1-1 recA3-3* plants and in other mutants affected in mtDNA recombination surveillance. Quantification of the EE parental genomic sequences and crossover products in the individual F1 plants revealed that all had undertaken sorting of the alternative genomes (Figure 8C). These results were reproduced in two independent backcross experiments. Among 76 F1 plants analyzed, one-third (26/76) had drastically reduced copy numbers of the recombined genomic sequences (deleted mtDNA sequence EE-1/2 and episome EE-2/1), while maintaining wild-type levels of the parental sequence EE-1/1-EE-2/2. An additional third of the plants (22/76) had intermediate levels of mtDNA reversion, with normal EE-1/1-EE-2/2 copy numbers and significant reduction of EE-1/2 and/or EE-2/1. The recombined genomic sequences showed a differential segregation in many plants, which confirmed that they were not genetically linked. The loss of EE-2/1 in revertants was thus not necessarily through recombination with EE-1/2, which should result in stoichiometric reduction of both sequences, but rather occurred by suppression of its replication or transmission.

The analysis of the F1 plants displaying variegated phenotypes showed that most had asymmetrically segregated the alternative EE sequences (Figure 8C), with simultaneous reduction of the two configurations carrying the *ATP1* gene (EE-1/1-EE-2/2 and episome EE-2/1). This suggested that the observed phenotype resulted from a reduction in ATP1 expression. Indeed, the reduction in copy number of the *ATP1* gene was confirmed in all variegated plants tested (Figure 9A). Moreover, quantification of *ATP1* in different leaves of a chimeric plant containing both normal-looking

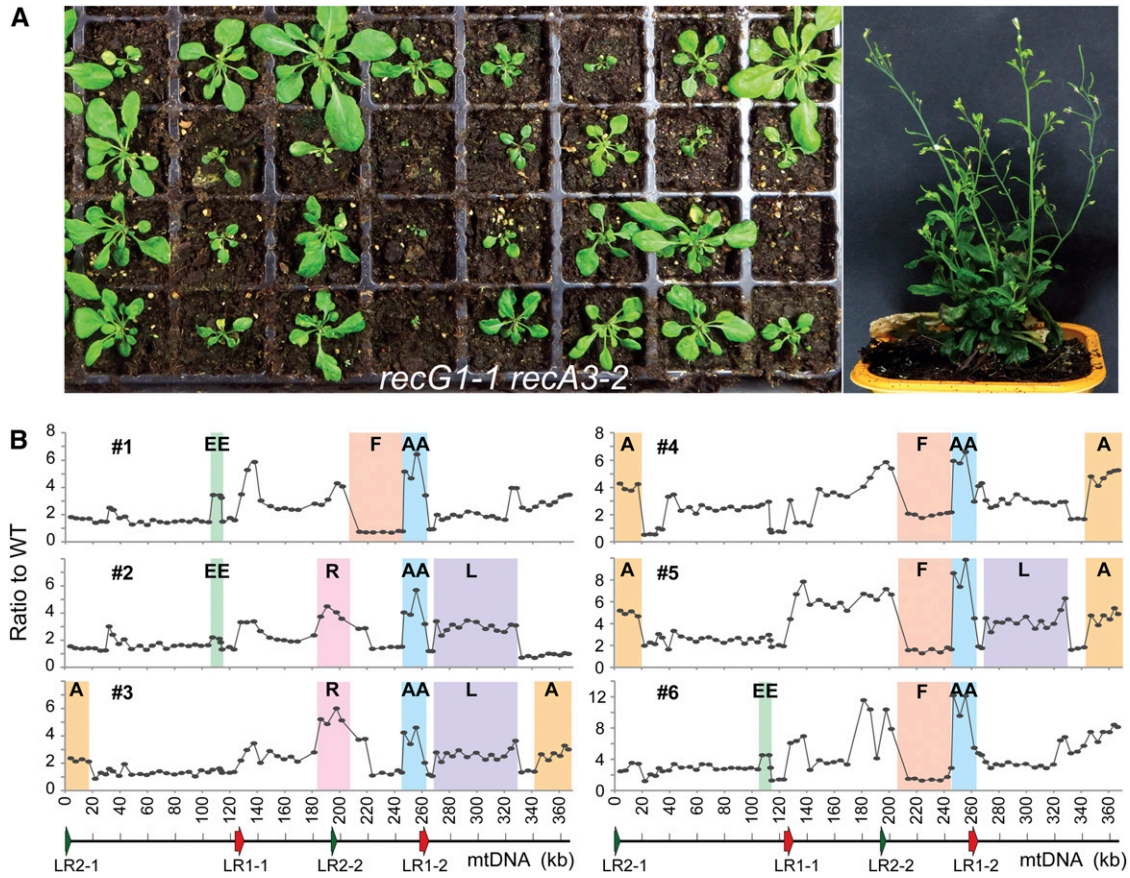

Figure 7. Synergistic Effect of *recG1* on *recA3*.

Knockdown of *RECG1* potentiates the *recA3* mutation, which results in plants that segregate different mitotypes resulting from recombination.
(A) Variable severity of the phenotypes developed by *recG1-1 recA3-2* double mutants. The plant on the right illustrates a severe phenotype of dwarfism, leaf distortion, variegation, and sterility.
(B) Changes in the copy number and stoichiometry of mtDNA sequences in individual *recG1-1 recA3-2* plants. The mtDNA was scanned for differences in copy number as described in Figure 6A. The linear representation of the Col-0 mtDNA is displayed below the graphics, with the coordinates in kilobases and the two pairs of large repeated sequences LR1 and LR2. Colored regions indicate sequences whose increase or decrease can be explained by the loop-out of subgenomes by recombination involving the indicated direct repeats, followed by their autonomous replication and/or segregation.

and variegated leaves (plant F1-51; Figure 8B) confirmed that the severity of the phenotype correlated with the reduction in *ATP1* (Figure 9A). The decrease in gene copy number also correlated with a significant reduction of the *ATP1* transcript (Figure 9B). Detection of the ATP1 protein in immunoblots of total leaf extracts showed that the *recG1*-2 mutant had normal or slightly higher amounts of ATP1 but that the protein was significantly reduced, by a factor of 2-fold, in the variegated plant F1-55 (Figure 9C). The limited reduction in protein compared with the dramatic reduction in gene transcript is possibly the result of the differential turnover rates. Therefore, the variegated phenotype apparently resulted from clonal asymmetrical segregation of the alternative mitotypes, with a compromised oxidative phosphorylation in tissues inheriting below-threshold levels of *ATP1*. To confirm this hypothesis, we measured the respiration capacity of normal and severely affected variegated leaves, of equivalent size and weight. We did indeed find that the affected tissues had much reduced respiration rates compared with normal leaves (Figure 9D).

Remarkably, among the F1 plants, a significant proportion (14/76) displayed completely shifted mtDNA genomes, having almost completely lost the wild-type genome (EE-1/1-EE-2/2) and retained the recombined forms EE-1/2 and EE-2/1. These plants had a new near-homoplasmic mtDNA and were phenotypically indistinguishable from wild-type plants. Hybridization to undigested DNA showed that the fast-migrating mtDNA form (the EE-2/1 episome) was lost in the F1 shifted plants (Figure 10A). The high molecular weight EE-2/1 configuration that was retained either corresponded to a head-to-tail concatemeric autonomous replicon or resulted from a reintegration of the EE-2/1 sequence into a new locus of the main genome. The latter hypothesis was confirmed by DNA restriction analysis, as well as by qPCR (Figure 10). According to these experiments, the EE-2/1 sequence reintegrated the genome through recombination involving the repeated sequence T, which is present just upstream of *ATP1* and is repeated elsewhere in the mtDNA (sequences T-1/1 and T2/2 respectively; Figure 10B). The product of this secondary

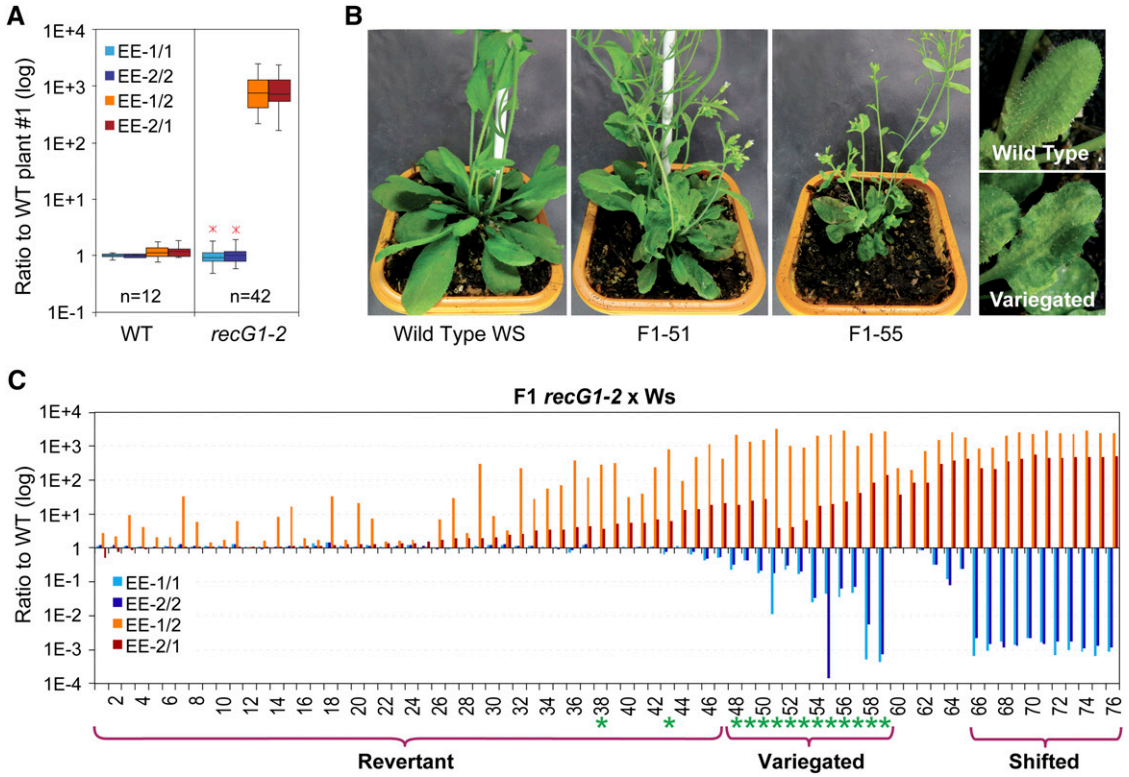

Figure 8. Backcross Triggers Genomic Shift Involving EE Repeats.

The stable mtDNA structure found in *recG1-2* knockout plants (Figure 6D) is destabilized by reintroduction of the RECG1 allele by backcross, resulting in segregation of plants with different mitotypes.

(A) Stable ratios of the sequences derived from repeats EE in wild-type and *recG1-2* plants. The values were compared with a same individual wild-type plant.

(B) Examples of F1 plants from backcross presenting phenotypes of leaf variegation and distortion.

(C) Analysis of the EE configurations, as in Figure 5, in 76 individual F1 plants. Green asterisks indicate plants displaying the variegation phenotypes shown in **(B)**. Revertants are plants that have significant reduction in the EE-2/1 subgenome containing sequence. Shifted plants are the ones that retain the EE-1/2 and EE-2/1 subgenomes and have nearly lost the EE-1/1 and EE-2/2 parental sequence.

recombination event is already present in homozygous *recG1-2* plants, giving a 5.4-kb diagnostic *Spe*I restriction fragment hybridizing with the *ATP1* internal probe (Figure 10A). This modified genome was preferentially segregated in the shifted plants, to the detriment of the wild-type mtDNA, which was virtually lost. The qPCR analysis supports this interpretation, showing a 9-fold increase of the T-1/2 and T2/1 recombined forms in shifted plant compared with homozygous *recG1-2* plants, with a corresponding loss of the T-1/1 and T-2/2 wild-type sequences (Figure 10C). Thus, our analysis shows that in *recG1-2* F1 plants, there was a differential segregation of three alternative mitotypes that were already present in the homozygous mutant: (1) the wild-type mtDNA, (2) the mitotype subdividing into the EE-1/2 form and the EE-2/1 episome, and (3) the mtDNA resulting from the reintegration of EE-2/1 into the main mtDNA by a secondary recombination event involving repeats T-1/1 and T-2/2.

Finally, analysis of the F2 generation of the shifted plants showed that the mtDNA remained stable in all *RECG1:recG1-2* and *RECG1:RECG1* plants, with no further changes in the ratios of the EE-containing configurations (Figure 10D). However, in all F2 *recG1:recG1* homozygous plants (13 plants analyzed), there was a remarkable reincrease of the parental EE-1/1-EE-2/2 sequence, by a factor of ~100-fold. Thus, in these plants, a new cycle of mtDNA changes by recombination was again elicited by the loss of RECG1.

DISCUSSION

Multiple Activities of RecG-Like Proteins

Our results show that RECG1 acts at multiple stages of mtDNA maintenance, both in recombination-dependent repair and in the surveillance of recombination activities that compromise the integrity of the organellar genomes. In addition, characterizing the segregation of the mitotypes coexisting in *recG1* plants allowed us to address the mechanisms underlying mtDNA stoichiometric shifting and to better understand how these can lead to stable novel mtDNA configurations.

According to our computer modeling, the plant RECG1 appears to be structurally homologous to bacterial RecG, which suggests that it shares similar activities. This is supported by the ability of the

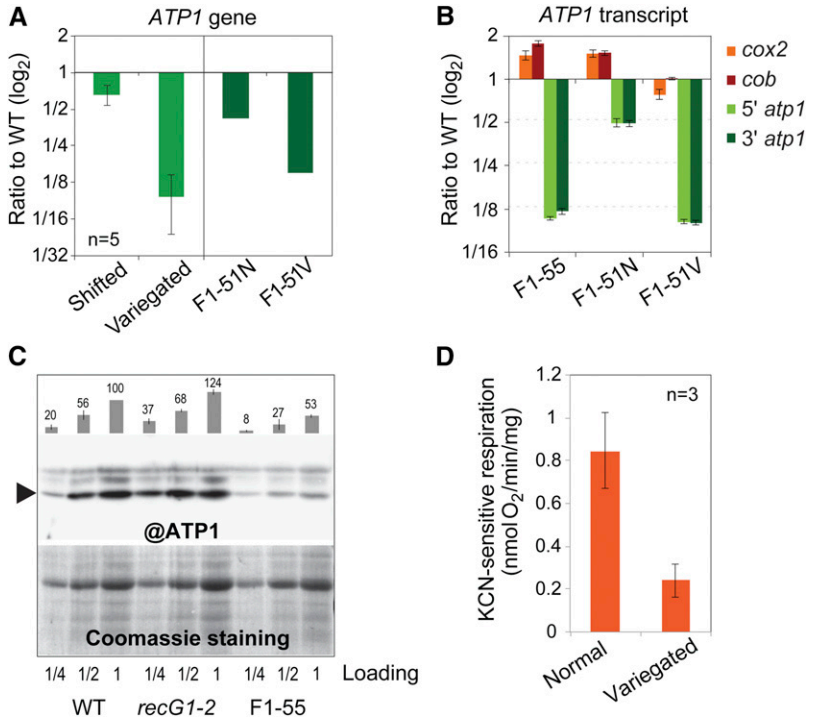

Figure 9. The Variegation Phenotypes Result from Reduced Transmission and Expression of the *ATP1* Gene.

(A) Correlation between variegation phenotypes and reduction in *ATP1* copy number in F1 plants. The results are the means and SD from five plants analyzed. The results obtained for a variegated leaf (V) and a normal leaf (N) from plant F1-51 are shown.

(B) As in **(A)**, but for the abundance of the *ATP1* transcript, compared with two other mtDNA-encoded genes. Two different *ATP1* sequences from the 5′ and 3′ parts of the gene were tested.

(C) Immunodetection and relative quantification of the ATP1 protein (@ATP1), showing a correlation between the affected phenotype of plant F1-55 and a reduced steady state level of ATP1 versus the wild type and *recG1-2*. The Coomassie blue staining of the membrane is shown as loading control. The arrowhead indicates the protein migrating at the expected size of 55 kD.

(D) Measure of the KCN-sensitive oxygen consumption in 3-week-old normal or variegated leaves.

plant sequence to replace the bacterial protein in all functional tests that we performed. One can speculate that the few extra sequences that are present in RECG1 might modulate plant-specific interactions and probably do not change the overall modular organization of the protein and its activity. Thus, RECG1 possibly has similar functions in plant organelles as RecG in bacteria.

Bacterial RecG has multiple roles in DNA metabolism and can target a plethora of different nucleic acid structures, including replication forks, HJs, D-loops, and R-loops (Supplemental Figure 5). RecG is associated with later stages of repair by recombination because of its ability to catalyze branch migration of HJs, as does RuvAB. But RecG is not redundant with RuvAB, since it has no associated nuclease activity that could resolve HJs, whereas RuvAB recruits the RuvC nuclease (Zhang et al., 2010). Analysis of recombination intermediates also revealed independent effects of *ruvAB* and *recG* mutations in the resolution of HJs (Mawer and Leach, 2014). As RecG in bacteria, in plant organelles, RECG1 should be able to translocate HJs and have major roles in their resolution. But in plants there are no orthologs of RuvABC, which conversely suggests that plant RECG1 can take over RuvAB functions. However, we found that RECG1 cannot complement *ruvAB* in bacteria, and functional homologs that act in the nucleus such as the RAD54 translocase and the GEN1 and SEND1 resolvases are apparently not targeted to organelles (Osakabe et al., 2006; Bauknecht and Kobbe, 2014). RECG1 should then perform in cooperation with a not yet identified resolvase. Alternatively, RECG1 alone might be able to eliminate HJs, simply by driving branch migration till they merge with replication forks, as has been suggested for bacterial RecG (Wardrope et al., 2009).

An additional major function of bacterial RecG is the suppression of replication initiation, associated with its ability to dissociate R-loops and D-loops. This allows RecG to repress replication of plasmids that require an RNA primer for replication initiation (Vincent et al., 1996; Fukuoh et al., 1997) and to suppress potentially pathological replication reinitiation, such as when converging replication forks meet (Rudolph et al., 2010, 2013). Our complementation results demonstrated that plant RECG1 can ensure such functions in bacteria, which suggests that it can dissociate R-loops and D-loops. As discussed below, such an activity could be responsible for the loss of the EE episome, when the *RECG1* allele is reintroduced by backcross. Finally, bacterial RecG can convert three-way to four-way DNA junctions, an ability that has mainly been associated with the rescue of stalled replication forks and the bypass of blocking

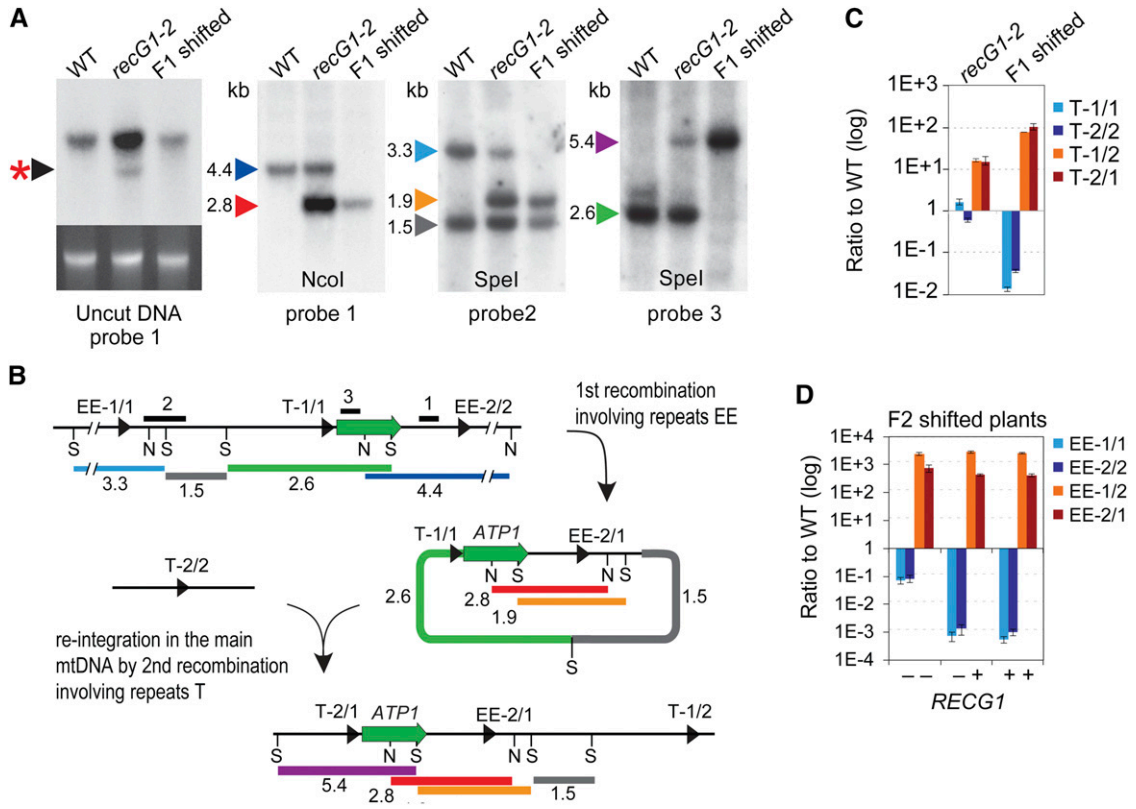

Figure 10. Genomic Shift Results in a New mtDNA Genome.

(A) and **(B)** DNA gel blot hybridizations **(A)** supporting the model **(B)** proposed to explain how F1-shifted plants inherited a new mtDNA configuration by reintegration of the EE-2/1 subgenome into a new genomic locus of the main mtDNA, via recombination involving repeats T-1/1 and T-2/2. The asterisk indicates the EE-2/1 replisome visible in uncut DNA of homozygous *recG1-2* and lost in shifted F1 plants. The arrowheads indicate hybridizing restriction fragments with a color code corresponding to the fragments represented in the explaining scheme. *Spe*I (S) and *Nco*I (N) sites are indicated. The thick black lines labeled 1, 2, and 3 indicate the sequences used as probes.

(C) Relative qPCR quantification of the parental configurations (T-1/1 and T2/2) of mitochondrial repeat T and of the corresponding crossover products (T-1/2 and T-2/1) in *recG1-2* and F1 shifted plants, as outlined in Figure 4C.

(D) Relative qPCR analysis of the EE sequences in the F2 progeny of F1-shifted plants. The genotype regarding the *recG1-2* mutation is indicated.

lesions (McGlynn and Lloyd, 2000; McGlynn et al., 2001). Whether RECG1 is involved in the rescue of stalled forks during replication of the organellar genomes remains to be established but would have implications discussed below.

Roles of RECG1 in Controlling Proper Homologous Recombination in Plant Organelles

We observed that Arabidopsis *recG1* mutants display several distinct molecular phenotypes. First, under unrestricted growth conditions, they accumulate mtDNA sequences generated by ectopic HR, in which IRs are used as loci of strand invasion (Figure 5). In wild-type plants, these ectopic recombination events are tightly suppressed. This same molecular phenotype has been observed in several other mutants, affected in the expression of unrelated proteins, including the RecA-like mitochondrial recombinases RECA2 and RECA3, the single-stranded DNA binding protein OSB1, and the MutS-like protein MSH1 (Zaegel et al., 2006; Arrieta-Montiel et al., 2009; Shedge et al., 2010; Miller-Messmer et al., 2012). This implies that these proteins participate in similar pathways of recombination and that when these pathways are compromised, there is activation of error-prone recombination activities that are normally repressed. These are most likely break-induced replication-related activities that result in increased ectopic recombination due to the repeat-rich mitochondrial genome of plants (Christensen, 2013). The pathways of recombination that are compromised in mutants of these proteins are RecA-dependent, since loss of either RECA2 or RECA3 also leads to the same molecular phenotype (Miller-Messmer et al., 2012).

Second, the *recG1* mutants are more sensitive to CIP treatment, which induces DSBs in the organellar genomes (Figure 4). Induction of HR-dependent mtDNA repair in wild-type plants also results in increased mobilization of IRs as possible sites of strand invasion. This effect is reduced in *recG1* plants, as it is in other mutants impaired in mtDNA repair by recombination (Janicka et al., 2012; Miller-Messmer et al., 2012). Therefore, it seems that the induction of DSBs by CIP treatment in wild-type lines

phenocopies the effect of mutations that induce ectopic recombination in regular growth conditions. It suggests that the effect of such mutations is an overall increase in mtDNA breaks that is mimicked by the genotoxic treatments. The increase could result from the inability to repair DNA lesions by break-avoiding pathways.

These pathways could be involved in the recovery of blocked replication forks. In organelles, the main threats to DNA integrity are modified bases and cross-links that are frequently generated in the oxidative environment of mitochondria and chloroplasts. Such lesions can block DNA polymerase progression, challenging the duplication of the organellar genomes. If the stalled forks cannot be rescued, by repair or bypass of the blocking lesion, the replisome might dissociate, resulting in fork collapse. Further DNA synthesis will then require recombination to restart replication (Supplemental Figure 6). It is probable that RECG1, like bacterial RecG, promotes fork regression to bypass unrepaired replication blocks. Other factors whose mutations result in increased ectopic recombination might also be required for efficient replication repair and restart of stalled replication forks, avoiding fork collapse. Conversely, failure to recover stalled forks in *recG1* or other mutants would result in DNA breaks. The broken DNA ends would then be recovered for replication restart by recombination through the break-induced replication pathway, which is error-prone and can give rise to gross rearrangements, copy number variations, and loss of sequence synteny if it occurs in the context of repeated sequences (Saini et al., 2013). This scenario can explain both the increase in ectopic recombination in *recG1* and other mutants and the phenocopy of mutation effects by drugs that induce DSBs, as discussed above. RecA-like proteins also promote replication fork reversal, in particular in the presence of single-strand gaps that result from the blocking of lagging strand progression (Robu et al., 2004; Cox, 2007). Contrarily, RecG should preferentially target forks blocked on the leading strand (Supplemental Figure 6). In the context of plant organelles, complementary and partially redundant functions of RecA proteins and RECG1 in the rescue of stalled replication could explain why (1) the single *recG1* mutation has a mild effect on organellar genome maintenance and does not impair normal plant growth, and (2) the double mutation *recG1-1 recA3-2* has a synergistic effect on the stoichiometric replication of the Arabidopsis mtDNA.

Finally, our results also suggest that RECG1 is able to displace D-loops and R-loops, an activity that allows bacterial RecG to selectively support recombination at locations with extensive DNA sequence homology (Vincent et al., 1996; Fukuoh et al., 1997). Indeed, it was shown in bacteria that recombination between correctly aligned sister sequences involves an unstable intermediate that is stabilized by RecG-dependent branch migration, which converts three-way to four-way DNA junctions (Mawer and Leach, 2014). It can thus be speculated that branch migration of D-loops catalyzed by RECG1 might help to discriminate between regions of limited or extensive sequence identity for strand invasion in plant mitochondria, preventing undesirable genomic rearrangements. The loss of RECG1 would in turn result in increased ectopic recombination.

No Significant Effect of RECG1 in the Maintenance of the cpDNA in Arabidopsis

RECG1 is apparently dually targeted to mitochondria and chloroplasts, as shown through both transient and constitutive expression of a GFP fusion protein in plants. The RECG1 promoter-GUS fusion results also showed important gene activity in photosynthetic tissues. It was therefore expected that RECG1 would exert the same functions in both organelles and affect the maintenance of both the mtDNA and the cpDNA. However, in *recG1* knockdown and knockout plants, we have not seen any significant effects on the copy number of the cpDNA, on the stoichiometry of the cpDNA regions, or on the surveillance of recombination mobilizing repeated sequences. These observations contrast with recently published results on the *P. patens* ortholog of RECG1, which is also dually targeted to both organelles and whose deletion caused an increase in recombination mobilizing mtDNA IRs of 47 to 79 bp, but also cpDNA IRs of 48 to 63 bp (Odahara et al., 2015). There are several possible explanations for these functional differences. First, it cannot be excluded that overexpression under the strong 35S promoter results in mistargeting of the GFP fusion protein into chloroplasts. Second, it has already been seen with dually targeted proteins that one location can be favored versus the other (Carrie and Whelan, 2013). That seems to be the case for Arabidopsis RECA2, which is dually targeted but appeared to affect only the maintenance of the mtDNA (Shedge et al., 2007; Miller-Messmer et al., 2012). Third, the organellar recombination machineries of *P. patens* and Arabidopsis show further differences, and not all intervening factors are shared between the two species. For instance, RECA3 and WHY proteins, which are important for organellar HR-dependent repair in Arabidopsis, are not found in *P. patens*. Finally, it is possible that the effects of RECG1 on the maintenance of the Arabidopsis cpDNA are not visible: Long IRs of more than 100 bp of perfect identity, which are fairly abundant in the Arabidopsis mtDNA and are the major sites of ectopic HR, are not present in the cpDNA. The chloroplast repeated sequence R2 that we monitored is a 76-bp imperfect repeat with five mismatches, whose two copies only share a stretch of 32 bp of perfect identity. It is therefore unlikely to constitute an efficient substrate for HR. In Arabidopsis mitochondria, efficient mobilization of such small repeats for recombination has not been observed (Davila et al., 2011). On the contrary, mitochondrial and chloroplastic repeated sequences that are active in ectopic HR in *P. patens* are essentially small (Odahara et al., 2009, 2015), definitely reflecting differences between the organellar recombination machineries of the two species. In this context, it might be noted that recombinational activities that reshuffle mtDNA gene arrangements only came with the onset of spermatophytes (Knoop, 2013). Finally, in CIP-treated wild-type plants we have seen that recombination involving R2 is significantly increased, indicating that this repeat can be efficiently mobilized during HR-dependent repair of cpDNA DSBs. However, the absence of RECG1 in mutant plants does not significantly affect this mobilization, suggesting that it is mediated by other factors.

Multiple Mitotypes in *recG1* Plants

In this study, we observed that in *recG1-2* plants the increased ectopic recombination produced an episome that apparently could replicate autonomously, resulting in the generation of two alternative genomes differing in a single locus. In the *recG1-2* background, there is a stable coexistence of these alternative

mitotypes, at least for two plant generations. It is not clear why additional autonomous subgenomes were not created in the mutant. One possible reason is that EE repeats are the IRs closest to each other in the mtDNA and that recombination involving repeats far apart is much less efficient. The small size of the EE-2/1 episome should also support a faster replication rate. How replication of the EE-2/1 episome initiates is not known, but the presence of the very actively transcribed *ATP1* gene might help, either by locally melting the DNA and facilitating strand invasion for recombination-dependent replication or by providing RNA primers for replication initiation. In *recG1-1 recA3-2* plants, we observed additional changes in the stoichiometry of several mtDNA regions, not occurring in single mutants and explainable by similar processes of recombination involving directly oriented IRs and independent replication of the resulting products. This synergistic effect of the *recG1-1* hypomorphic mutation and the *recA3* knockout mutation implies that the two genes act in partially redundant pathways that control the correct stoichiometric transmission of the mtDNA. Independent and preferential replication explains how these sequences that are generated in somatic tissues at relatively low frequencies can become predominant. While qPCR data show that virtually all pairs of IRs are targets of increased ectopic recombination, only a few of them promote significant changes in the copy number of the sequences comprised between the repeats. These might be the few recombination products that are able to replicate and segregate autonomously.

A Model for mtDNA Segregation and Stoichiometric Shifting

The alternative mitotypes discussed above segregated in the F1 plants of the *recG1-2* backcross, after reintroduction of the *RECG1* allele. The analysis of these events allowed us to understand characteristics of stoichiometric shifting and generation of a new stable mtDNA structure compatible with normal plant development. We could also directly link phenotypes of leaf distortion and variegation to a reduced expression of a gene essential for oxidative phosphorylation. The subpopulation of F1 plants that we classified as variegated developed specific developmental phenotypes that also occur in several other Arabidopsis mutants impaired in mitochondrial recombination functions (Sakamoto et al., 1996; Zaegel et al., 2006; Arrieta-Montiel et al., 2009). As we observed, these phenotypes are also widespread in *recG1-1 recA3-2* plants. In mutant and double mutant plants that have been previously described, the penetrance and severity of phenotypes correlated with increased mtDNA rearrangements by recombination. However, given the variability and extension of the mtDNA changes in those plants, it has not been possible to directly link phenotypes to specific changes in organellar gene expression. On the contrary, in the variegated F1 plants, the phenotypes clearly correlated with the loss of the *ATP1* gene and the reduction of the corresponding transcript. This should result in a significant decrease in ATP1 protein and oxidative phosphorylation. Thus, we show here that the likely explanation for these phenotypes is the loss of mtDNA regions coding for genes essential to OXPHOS functions. The clonal tissue distribution, with regions that are more or less affected depending on the differential inheritance of the deleted mtDNA, recalls what has been observed in NCS (nonchromosomal stripe) maize (*Zea mays*) mutants (Gu et al., 1993).

In the *recG1-2* F1 plants, there was a segregation of mtDNA mitotypes that was not observed in homozygous *recG1-2*, at least up to generation T5. Therefore, it seems that sorting of the alternative mitotypes coexisting in *recG1-2* was not possible in the absence of the *RECG1* allele. In almost all segregating F1 plants, the sorting of the alternative mitotypes correlated with a highly reduced copy number of the EE-2/1 episome, either because of its loss in revertants or because of its integration into the mtDNA by secondary recombination in the shifted plants. This suggests that sorting was contingent on the ability of mitochondria to lose the EE-2/1 episome, in a RECG1-dependent manner. That could be because of multiple reasons. The ability of RECG1 to dissociate D-loops or R-loops could explain how its reintroduction by backcross suppresses the replication of the episome. As we have shown, expression of RECG1 in bacteria is able to repress the copy number of ColE1-dependent plasmids, which require an RNA primer for replication initiation. Indeed, one of the possible functions of RECG1 in mitochondria could be to suppress replication of aberrant mtDNA sequences, if the process involves an R- or D-loop. Another possible explanation is that the EE episome might be catenated with the main mtDNA molecules, from which it cannot dissociate during replication in the absence of RECG1. As we have seen, a major part of the EE-2/1 sequence in *recG1-2* comigrates with high molecular weight DNA. It can be hypothesized that these sequences would correspond to duplications in the main mtDNA genome. However, in that case, we would not expect to see a reduction of the EE-1/1 and EE-2/2 sequences compared with the neighboring mtDNA regions, as it was observed (Figures 5A and 6B). A possible catenation of the EE-2/1 episome better explains these results. Therefore, it is possible that RECG1 cooperates in the decatenation of the DNA, as it has already been described for other helicases (Ramamoorthy et al., 2012).

Finally, our backcross experiments generated shifted plants with a stable rearranged mtDNA, differing from the original mtDNA by the transposition of a specific sequence to a different locus. This study gave us a comprehensive scenario of how the mtDNA can rapidly evolve by stoichiometric shifting, in two steps (Figure 9B). First, recombination involving directly oriented IRs engenders subgenomes whose copy number significantly increases by autonomous replication. In a second step, the high copy number reached by these subgenomes favors additional recombination events that permit their reintegration into a different locus of the main genome, changing the structural organization of the mtDNA sequences. Factors such as RECG1 modulate such processes, by controlling the recombination frequency and the replication of subgenomes.

METHODS

Plant Material and Growth Conditions

Arabidopsis thaliana T-DNA insertion lines *recG1-1* (WiscDsLox485-488E5) and *recG1-2* (FLAG_630A09) were obtained from the Nottingham Arabidopsis Stock Centre and from the Versailles Arabidopsis Stock Centre, respectively. Plants were grown on soil or in vitro at 23°C under

a 16-h light photoperiod. For in vitro cultures, surface-sterilized seeds were sown on agar plates containing MS255 (Duchefa) supplemented with 1% (w/v) sucrose and stratified during 3 d at 4°C.

Phylogenetic Analysis

Bacterial and plant sequences were identified in the databases using the *Escherichia coli* RecG sequence as query. An alignment was constructed with ClustalW implemented in the MacVector package using the GonneT matrix. Phylogenetic trees were built with the PhyML v3.1 online software (www.phylogeny.fr; Dereeper et al., 2008) using the neighbor-joining method implemented in the BioNJ program and 100 bootstrap support. Graphical representations were performed with TreeDyn (v198.3).

E. coli Complementation Assays

The *E. coli* DH5α strain was used for routine cloning, whereas the JM103 (*recG*+ and *ruvA*+), JM103 *recG::kan* (Δ*recG*), and JM103 *ruvA::Tc* (Δ*ruvA*) strains were used for complementation assays. The *RECG1* cDNA without targeting sequence (codons 58 to 957) was synthesized (http://www.genecust.com) and transferred into the *Pac*I and *Asc*I restriction sites of *pACYClacz* under the control of the isopropyl β-D-1-thiogalactopyranoside (IPTG)-inducible *lac* promoter. (Miller-Messmer et al., 2012). Codons were adapted to tRNA frequency in bacteria. The resulting construct was introduced in Δ*recG* and Δ*ruvA* strains, and complementation results were compared with wild-type and mutant strains transformed with the empty *pACYClacz* vector. Induced expression of the recombinant protein was monitored with a polyclonal antibody directed against RECG1. To raise the antibody, the sequence corresponding to the last 260 C-terminal amino acids of Arabidopsis RECG1 was cloned into the p0GWA expression vector (Busso et al., 2005). The recombinant protein containing a C-terminal His-tag was expressed in the Rosetta(DE3)pLysS *E. coli* strain (Novagen), purified under denaturing conditions on Ni-NTA agarose (Qiagen), and injected into rabbits.

For DNA repair assays, 5 mL of Lysogeny broth supplemented with 1% (w/v) glucose and 10 μg/mL chloramphenicol was inoculated with 25 μL of overnight cultures and bacteria were grown at 37°C. Expression of RECG1 was induced at A_{650} = 0.2 by the addition of 0.25 mM IPTG and bacteria further grown till A_{650} = 0.4. Appropriate dilutions were spread on Lysogeny broth plates in triplicate and exposed to different UV-C doses (checked with an UV radiometer) before incubation at 37°C in the dark. The colony-forming units were counted and survival was calculated relative to the minus UV control.

For the overreplication complementation assays, cultures were grown to A_{650} = 1.2, diluted 400-fold with chloramphenicol-containing medium plus 0.25 mM IPTG, and further grown at 37°C. Samples at exponential growth were taken at A_{650} = 0.4 and A_{650} = 1.0 (~3 and 4 h after inoculation). Samples at the stationary phase were taken several hours after the A_{650} was stable. DNA was extracted with the Gene Elute Bacteria kit (Sigma-Aldrich), and the relative copy numbers of the sequences corresponding to *OriC*, *TerA*, *TerB*, and to the *YdcR* gene (located equidistantly between *TerA* and *TerB*) were determined by qPCR. Results were normalized against the mean of *TerA* and *TerB*. When analyzing the effect of RECG1 expression on the replication of the pBAD/Thio (Invitrogen) and pUC19 (NEB) plasmids, the relative plasmid copy numbers between exponentially growing cultures and saturated precultures were compared, and results were normalized against the *TerA* sequence.

Intracellular Localization and RECG1 Promoter-GUS Fusion

For in vivo intracellular localization, the sequence encoding the N terminus of RECG1 up to the region conserved in all RecG sequences (the first 208 codons) was cloned into the pCK-GFP3 vector, upstream and in frame with the GFP coding sequence, under the control of the CaMV 35S promoter, and young leaves of *Nicotiana benthamiana* were transfected by bombardment as described before (Vermel et al., 2002). The pCKmRFP plasmid (Vermel et al., 2002) was cotransfected as an internal mitochondrial marker. After 24 h, the fluorescence of GFP and chlorophyll was observed at 505 to 540 nm and beyond 650 nm, respectively, after excitation at 488 nm on a Zeiss LSM700 confocal microscope. The DsRED fluorescence was excited at 555 nm and observed at 560 to 615 nm. For constitutive expression in Arabidopsis, the expressing cassette was transferred from pCK-GFP3 into the *Asc*I and *Pac*I restriction sites of pBINPlus (van Engelen et al., 1995), and Arabidopsis Col-0 plants were transformed by the floral dip method. Leaves of selected transformants were observed at the confocal microscope at different stages of development. For promoter-GUS histochemical analysis, the 5′ upstream region of *RECG1* (595 nucleotides, starting just after the upstream gene and comprising 161 nucleotides of *RECG1* 5′-UTR) was cloned upstream of the *GUS* gene in the binary vector pMDC162 (Curtis and Grossniklaus, 2003), and the construct was used to generate stable Arabidopsis transformants. Tissues from six independent lines were stained with 5-bromo-4-chloro-3-indolyl-β-glucuronic acid (X-Gluc; Biosynth) as described (Zaegel et al., 2006) and observed by stereomicroscopy and transmission microscopy.

DNA Gel Blots, Genotoxic Stress Treatments, and Immunoblots

Genomic DNA was extracted using the cetyltrimethylammonium bromide method (Murray and Thompson, 1980). Plant genotypes were determined by PCR using gene- and T-DNA-specific primers. Total RNA was extracted with TRIzol (Life Technologies). For genotoxic stress assays, seeds were surface sterilized and spread on MS255 1% sucrose plates supplemented with different concentrations of ciprofloxacin (Sigma-Aldrich). Pools of 10 plants were harvested at 10 d, and total DNA was extracted for further analysis. For immunoblots, total leaf proteins were extracted in the presence of 2% (w/v) SDS and 4 M urea and precipitated with methanol-chloroform before SDS-PAGE fractionation and transfer to Immobilon-P membranes. The ATP1 protein was detected with an antiserum raised against the α-subunit of the mitochondrial ATP synthase from yeast. Chemiluminescence was quantified with a Fusion-FX7 camera system (Vilber Lourmat). Respiration capacity was measured in an Oxygraph oxygen electrode (Hansatech Instruments) in young 3-week-old leaves. The rates of oxygen consumption were measured after tissue addition and subtracted from the rates after addition of KCN.

qPCR Analysis

qPCR assays were performed in a LightCycler480 (Roche), in 6 μL of reaction containing 1× LightCycler480 SYBR Green I Master Mix (Roche) and 0.5 μM of each primer. The thermocycling program was as follows: a 7-min denaturing step at 95°C, then 40 cycles of 10 s at 95°C, 15 s at 58°C, and 15 s at 72°C. The second derivative maximum method was used to determine Cp values, and PCR efficiencies were determined from DNA serial dilution curves or using LinRegPCR software (http://LinRegPCR.nl). Three technical replicates were performed for each experiment. The numbers of biological replicates are indicated in the figures. To measure the accumulation of ectopic recombination in mtDNA and cpDNA, primers flanking each repeat were used, as described in Figure 4C. The *COX2* (AtMG00160) and 18S rRNA (AtMG01390) mitochondrial genes and the 16S rRNA (AtCG00920) chloroplast gene were used for normalization. For quantification of mtDNA and cpDNA copy numbers, a set of primers located along the organellar genomes was used, and results were normalized against the *UBQ10* (At4G05320) and *ACT1* (At2G37620) nuclear genes. For RT-qPCR experiments, the *GAPDH* (At1G13440) and *ACT2* (At3G18780) transcripts were used as standards.

Modeling of the RECG1 Structure

Plant RECG1 sequences were aligned using ClustalX (Thompson et al., 1997). The Arabidopsis RECG1 sequence was modeled on the structure of *Thermotoga maritima* RecG bound to a three-way DNA junction

(pdb1GM5), using Modeler (Sali and Blundell, 1993; http://salilab.org/modeller/about_modeller.html). The score and E-value between the two sequences is 370 and 7e-114, respectively. Three insertions found in all plant RECG1 sequences have no equivalents in bacterial sequences and could not be modeled accurately. No constraints were imposed and these additional sequences were displayed as loops and hand-edited to adjust to figure size.

Accession Numbers

Sequence data from this article can be found in the Arabidopsis Genome Initiative or GenBank/EMBL databases under the following accession numbers: *RECG1*, At2g01440; *RECA3*, At3g10140; and *ATP1*, AtMg01190. Accession numbers of the sequences used for phylogenetic analysis are given in Supplemental Data Set 1.

Supplemental Data

Supplemental Figure 1. Phylogenetic tree of RecG proteins.

Supplemental Figure 2. Alignment of plant RECG1 protein sequences.

Supplemental Figure 3. Analysis of representative intermediate size repeats in accessions Col-0 and Ws.

Supplemental Figure 4. Scanning of the cpDNA of *recG1* mutants for changes in relative copy numbers of the different cpDNA regions.

Supplemental Figure 5. Activities catalyzed by bacterial RecG in genome maintenance.

Supplemental Figure 6. Recovery of blocked replication forks by RecG and RecA complementary functions.

Supplemental Table 1. Oligonucleotide primers.

Supplemental Data Set 1. Text file of alignment used for phylogenetic analysis.

ACKNOWLEDGMENTS

We thank Géraldine Bonnard for providing ATP1 antibodies and Jean Molinier and Marie-Edith Chaboute for helpful discussions. This work has been published under the framework of the LABEX [ANR-11-LABX-0057_MITOCROSS] and benefits from a funding from the state managed by the French National Research Agency as part of the "Investments for the Future" program.

AUTHOR CONTRIBUTIONS

C.W., M.L.R., and J.M.G. performed research. M. Bergdoll constructed the protein model. C.W., M. Bichara, A.D., and J.M.G. designed the research and analyzed data. C.W., A.D., and J.M.G. wrote the article.

Received July 31, 2015; revised September 14, 2015; accepted September 25, 2015; published October 13, 2015.

REFERENCES

Allen, J.O., et al. (2007). Comparisons among two fertile and three male-sterile mitochondrial genomes of maize. Genetics **177:** 1173–1192.

Alverson, A.J., Rice, D.W., Dickinson, S., Barry, K., and Palmer, J.D. (2011). Origins and recombination of the bacterial-sized multichromosomal mitochondrial genome of cucumber. Plant Cell **23:** 2499–2513.

Arrieta-Montiel, M.P., Shedge, V., Davila, J., Christensen, A.C., and Mackenzie, S.A. (2009). Diversity of the Arabidopsis mitochondrial genome occurs via nuclear-controlled recombination activity. Genetics **183:** 1261–1268.

Backert, S., and Börner, T. (2000). Phage T4-like intermediates of DNA replication and recombination in the mitochondria of the higher plant *Chenopodium album* (L.). Curr. Genet. **37:** 304–314.

Backert, S., Dörfel, P., Lurz, R., and Börner, T. (1996). Rolling-circle replication of mitochondrial DNA in the higher plant *Chenopodium album* (L.). Mol. Cell. Biol. **16:** 6285–6294.

Backert, S., Nielsen, B.L., and Borner, T. (1997). The mystery of the rings: structure and replication of mitochondrial genomes from higher plants. Trends Plant Sci. **2:** 477–483.

Bauknecht, M., and Kobbe, D. (2014). AtGEN1 and AtSEND1, two paralogs in Arabidopsis, possess holliday junction resolvase activity. Plant Physiol. **166:** 202–216.

Bellaoui, M., Martin-Canadell, A., Pelletier, G., and Budar, F. (1998). Low-copy-number molecules are produced by recombination, actively maintained and can be amplified in the mitochondrial genome of Brassicaceae: relationship to reversion of the male sterile phenotype in some cybrids. Mol. Gen. Genet. **257:** 177–185.

Briggs, G.S., Mahdi, A.A., Weller, G.R., Wen, Q., and Lloyd, R.G. (2004). Interplay between DNA replication, recombination and repair based on the structure of RecG helicase. Philos. Trans. R. Soc. Lond. B Biol. Sci. **359:** 49–59.

Busso, D., Delagoutte-Busso, B., and Moras, D. (2005). Construction of a set Gateway-based destination vectors for high-throughput cloning and expression screening in *Escherichia coli*. Anal. Biochem. **343:** 313–321.

Cappadocia, L., Maréchal, A., Parent, J.S., Lepage, E., Sygusch, J., and Brisson, N. (2010). Crystal structures of DNA-Whirly complexes and their role in Arabidopsis organelle genome repair. Plant Cell **22:** 1849–1867.

Carles-Kinch, K., George, J.W., and Kreuzer, K.N. (1997). Bacteriophage T4 UvsW protein is a helicase involved in recombination, repair and the regulation of DNA replication origins. EMBO J. **16:** 4142–4151.

Carrie, C., and Whelan, J. (2013). Widespread dual targeting of proteins in land plants: when, where, how and why. Plant Signal. Behav. **8:** e25034.

Chen, J., Guan, R., Chang, S., Du, T., Zhang, H., and Xing, H. (2011). Substoichiometrically different mitotypes coexist in mitochondrial genomes of *Brassica napus* L. PLoS One **6:** e17662.

Christensen, A.C. (2013). Plant mitochondrial genome evolution can be explained by DNA repair mechanisms. Genome Biol. Evol. **5:** 1079–1086.

Cox, M.M. (2007). Motoring along with the bacterial RecA protein. Nat. Rev. Mol. Cell Biol. **8:** 127–138.

Curtis, M.D., and Grossniklaus, U. (2003). A gateway cloning vector set for high-throughput functional analysis of genes in planta. Plant Physiol. **133:** 462–469.

Dasgupta, S., Masukata, H., and Tomizawa, J. (1987). Multiple mechanisms for initiation of ColE1 DNA replication: DNA synthesis in the presence and absence of ribonuclease H. Cell **51:** 1113–1122.

Davila, J.I., Arrieta-Montiel, M.P., Wamboldt, Y., Cao, J., Hagmann, J., Shedge, V., Xu, Y.Z., Weigel, D., and Mackenzie, S.A. (2011). Double-strand break repair processes drive evolution of the mitochondrial genome in Arabidopsis. BMC Biol. **9:** 64.

Dereeper, A., Guignon, V., Blanc, G., Audic, S., Buffet, S., Chevenet, F., Dufayard, J.F., Guindon, S., Lefort, V., Lescot,

M., Claverie, J.M., and Gascuel, O. (2008). Phylogeny.fr: robust phylogenetic analysis for the non-specialist. Nucleic Acids Res. **36:** W465–W469.

Diray-Arce, J., Liu, B., Cupp, J.D., Hunt, T., and Nielsen, B.L. (2013). The Arabidopsis At1g30680 gene encodes a homologue to the phage T7 gp4 protein that has both DNA primase and DNA helicase activities. BMC Plant Biol. **13:** 36.

Dudas, K.C., and Kreuzer, K.N. (2001). UvsW protein regulates bacteriophage T4 origin-dependent replication by unwinding R-loops. Mol. Cell. Biol. **21:** 2706–2715.

Feng, X., Kaur, A.P., Mackenzie, S.A., and Dweikat, I.M. (2009). Substoichiometric shifting in the fertility reversion of cytoplasmic male sterile pearl millet. Theor. Appl. Genet. **118:** 1361–1370.

Fukuoh, A., Iwasaki, H., Ishioka, K., and Shinagawa, H. (1997). ATP-dependent resolution of R-loops at the ColE1 replication origin by *Escherichia coli* RecG protein, a Holliday junction-specific helicase. EMBO J. **16:** 203–209.

Gerhold, J.M., Aun, A., Sedman, T., Jõers, P., and Sedman, J. (2010). Strand invasion structures in the inverted repeat of *Candida albicans* mitochondrial DNA reveal a role for homologous recombination in replication. Mol. Cell **39:** 851–861.

Gu, J., Miles, D., and Newton, K.J. (1993). Analysis of leaf sectors in the NCS6 mitochondrial mutant of maize. Plant Cell **5:** 963–971.

Gualberto, J.M., Mileshina, D., Wallet, C., Niazi, A.K., Weber-Lotfi, F., and Dietrich, A. (2014). The plant mitochondrial genome: dynamics and maintenance. Biochimie **100:** 107–120.

Janicka, S., Kühn, K., Le Ret, M., Bonnard, G., Imbault, P., Augustyniak, H., and Gualberto, J.M. (2012). A RAD52-like single-stranded DNA binding protein affects mitochondrial DNA repair by recombination. Plant J. **72:** 423–435.

Janska, H., Sarria, R., Woloszynska, M., Arrieta-Montiel, M., and Mackenzie, S.A. (1998). Stoichiometric shifts in the common bean mitochondrial genome leading to male sterility and spontaneous reversion to fertility. Plant Cell **10:** 1163–1180.

Kanazawa, A., Tsutsumi, N., and Hirai, A. (1994). Reversible changes in the composition of the population of mtDNAs during dedifferentiation and regeneration in tobacco. Genetics **138:** 865–870.

Kmiec, B., Woloszynska, M., and Janska, H. (2006). Heteroplasmy as a common state of mitochondrial genetic information in plants and animals. Curr. Genet. **50:** 149–159.

Knoll, A., and Puchta, H. (2011). The role of DNA helicases and their interaction partners in genome stability and meiotic recombination in plants. J. Exp. Bot. **62:** 1565–1579.

Knoop, V. (2013). Plant mitochondrial genome peculiarities evolving in the earliest vascular plant lineages. J. Syst. Evol. **51:** 1–12.

Lepage, É., Zampini, É., and Brisson, N. (2013). Plastid genome instability leads to reactive oxygen species production and plastid-to-nucleus retrograde signaling in Arabidopsis. Plant Physiol. **163:** 867–881.

Lloyd, R.G. (1991). Conjugational recombination in resolvase-deficient ruvC mutants of *Escherichia coli* K-12 depends on recG. J. Bacteriol. **173:** 5414–5418.

Lloyd, R.G., and Buckman, C. (1991). Genetic analysis of the recG locus of Escherichia coli K-12 and of its role in recombination and DNA repair. J. Bacteriol. **173:** 1004–1011.

Mahdi, A.A., Briggs, G.S., Sharples, G.J., Wen, Q., and Lloyd, R.G. (2003). A model for dsDNA translocation revealed by a structural motif common to RecG and Mfd proteins. EMBO J. **22:** 724–734.

Manosas, M., Perumal, S.K., Bianco, P.R., Ritort, F., Benkovic, S.J., and Croquette, V. (2013). RecG and UvsW catalyse robust DNA rewinding critical for stalled DNA replication fork rescue. Nat. Commun. **4:** 2368. Erratum. Nat. Commun. **5:** 4210.

Maréchal, A., and Brisson, N. (2010). Recombination and the maintenance of plant organelle genome stability. New Phytol. **186:** 299–317.

Matera, J.T., Monroe, J., Smelser, W., Gabay-Laughnan, S., and Newton, K.J. (2011). Unique changes in mitochondrial genomes associated with reversions of S-type cytoplasmic male sterility in maizemar. PLoS One **6:** e23405.

Mawer, J.S., and Leach, D.R. (2014). Branch migration prevents DNA loss during double-strand break repair. PLoS Genet. **10:** e1004485.

McGlynn, P., and Lloyd, R.G. (2000). Modulation of RNA polymerase by (p)ppGpp reveals a RecG-dependent mechanism for replication fork progression. Cell **101:** 35–45.

McGlynn, P., and Lloyd, R.G. (2002). Genome stability and the processing of damaged replication forks by RecG. Trends Genet. **18:** 413–419.

McGlynn, P., Lloyd, R.G., and Marians, K.J. (2001). Formation of Holliday junctions by regression of nascent DNA in intermediates containing stalled replication forks: RecG stimulates regression even when the DNA is negatively supercoiled. Proc. Natl. Acad. Sci. USA **98:** 8235–8240.

Meddows, T.R., Savory, A.P., and Lloyd, R.G. (2004). RecG helicase promotes DNA double-strand break repair. Mol. Microbiol. **52:** 119–132.

Miller-Messmer, M., Kühn, K., Bichara, M., Le Ret, M., Imbault, P., and Gualberto, J.M. (2012). RecA-dependent DNA repair results in increased heteroplasmy of the Arabidopsis mitochondrial genome. Plant Physiol. **159:** 211–226.

Mower, J.P., Touzet, P., Gummow, J.S., Delph, L.F., and Palmer, J.D. (2007). Extensive variation in synonymous substitution rates in mitochondrial genes of seed plants. BMC Evol. Biol. **7:** 135.

Murray, M.G., and Thompson, W.F. (1980). Rapid isolation of high molecular weight plant DNA. Nucleic Acids Res. **8:** 4321–4325.

Odahara, M., Kuroiwa, H., Kuroiwa, T., and Sekine, Y. (2009). Suppression of repeat-mediated gross mitochondrial genome rearrangements by RecA in the moss *Physcomitrella patens*. Plant Cell **21:** 1182–1194.

Odahara, M., Masuda, Y., Sato, M., Wakazaki, M., Harada, C., Toyooka, K., and Sekine, Y. (2015). RECG maintains plastid and mitochondrial genome stability by suppressing extensive recombination between short dispersed repeats. PLoS Genet. **11:** e1005080.

Oldenburg, D.J., and Bendich, A.J. (1996). Size and structure of replicating mitochondrial DNA in cultured tobacco cells. Plant Cell **8:** 447–461.

Osakabe, K., Abe, K., Yoshioka, T., Osakabe, Y., Todoriki, S., Ichikawa, H., Hohn, B., and Toki, S. (2006). Isolation and characterization of the RAD54 gene from *Arabidopsis thaliana*. Plant J. **48:** 827–842.

Parent, J.S., Lepage, E., and Brisson, N. (2011). Divergent roles for the two PolI-like organelle DNA polymerases of Arabidopsis. Plant Physiol. **156:** 254–262.

Ramamoorthy, M., Tadokoro, T., Rybanska, I., Ghosh, A.K., Wersto, R., May, A., Kulikowicz, T., Sykora, P., Croteau, D.L., and Bohr, V.A. (2012). RECQL5 cooperates with Topoisomerase II alpha in DNA decatenation and cell cycle progression. Nucleic Acids Res. **40:** 1621–1635.

Robu, M.E., Inman, R.B., and Cox, M.M. (2004). Situational repair of replication forks: roles of RecG and RecA proteins. J. Biol. Chem. **279:** 10973–10981.

Rowan, B.A., Oldenburg, D.J., and Bendich, A.J. (2010). RecA maintains the integrity of chloroplast DNA molecules in Arabidopsis. J. Exp. Bot. **61:** 2575–2588.

Rudolph, C.J., Upton, A.L., Briggs, G.S., and Lloyd, R.G. (2010). Is RecG a general guardian of the bacterial genome? DNA Repair (Amst.) **9:** 210–223.

Rudolph, C.J., Upton, A.L., Stockum, A., Nieduszynski, C.A., and Lloyd, R.G. (2013). Avoiding chromosome pathology when replication forks collide. Nature **500:** 608–611.

Saini, N., Ramakrishnan, S., Elango, R., Ayyar, S., Zhang, Y., Deem, A., Ira, G., Haber, J.E., Lobachev, K.S., and Malkova, A. (2013). Migrating bubble during break-induced replication drives conservative DNA synthesis. Nature **502:** 389–392.

Sakai, T., and Imamura, J. (1992). Alteration of mitochondrial genomes containing atpA genes in the sexual progeny of cybrids between *Raphanus sativus* cms line and *Brassica napus* cv. Westar. Theor. Appl. Genet. **84:** 923–929.

Sakamoto, W., Kondo, H., Murata, M., and Motoyoshi, F. (1996). Altered mitochondrial gene expression in a maternal distorted leaf mutant of Arabidopsis induced by chloroplast mutator. Plant Cell **8:** 1377–1390.

Sali, A., and Blundell, T.L. (1993). Comparative protein modelling by satisfaction of spatial restraints. J. Mol. Biol. **234:** 779–815.

Shedge, V., Arrieta-Montiel, M., Christensen, A.C., and Mackenzie, S.A. (2007). Plant mitochondrial recombination surveillance requires unusual RecA and MutS homologs. Plant Cell **19:** 1251–1264.

Shedge, V., Davila, J., Arrieta-Montiel, M.P., Mohammed, S., and Mackenzie, S.A. (2010). Extensive rearrangement of the Arabidopsis mitochondrial genome elicits cellular conditions for thermotolerance. Plant Physiol. **152:** 1960–1970.

Singleton, M.R., Scaife, S., and Wigley, D.B. (2001). Structural analysis of DNA replication fork reversal by RecG. Cell **107:** 79–89.

Sloan, D.B., Alverson, A.J., Chuckalovcak, J.P., Wu, M., McCauley, D.E., Palmer, J.D., and Taylor, D.R. (2012). Rapid evolution of enormous, multichromosomal genomes in flowering plant mitochondria with exceptionally high mutation rates. PLoS Biol. **10:** e1001241.

Small, I., Suffolk, R., and Leaver, C.J. (1989). Evolution of plant mitochondrial genomes via substoichiometric intermediates. Cell **58:** 69–76.

Thompson, J.D., Gibson, T.J., Plewniak, F., Jeanmougin, F., and Higgins, D.G. (1997). The CLUSTAL_X windows interface: flexible strategies for multiple sequence alignment aided by quality analysis tools. Nucleic Acids Res. **25:** 4876–4882.

van Engelen, F.A., Molthoff, J.W., Conner, A.J., Nap, J.P., Pereira, A., and Stiekema, W.J. (1995). pBINPLUS: an improved plant transformation vector based on pBIN19. Transgenic Res. **4:** 288–290.

Vermel, M., Guermann, B., Delage, L., Grienenberger, J.M., Maréchal-Drouard, L., and Gualberto, J.M. (2002). A family of RRM-type RNA-binding proteins specific to plant mitochondria. Proc. Natl. Acad. Sci. USA **99:** 5866–5871.

Vincent, S.D., Mahdi, A.A., and Lloyd, R.G. (1996). The RecG branch migration protein of *Escherichia coli* dissociates R-loops. J. Mol. Biol. **264:** 713–721.

Wall, M.K., Mitchenall, L.A., and Maxwell, A. (2004). Arabidopsis thaliana DNA gyrase is targeted to chloroplasts and mitochondria. Proc. Natl. Acad. Sci. USA **101:** 7821–7826.

Wardrope, L., Okely, E., and Leach, D. (2009). Resolution of joint molecules by RuvABC and RecG following cleavage of the *Escherichia coli* chromosome by EcoKI. PLoS One **4:** e6542.

Zaegel, V., Guermann, B., Le Ret, M., Andrés, C., Meyer, D., Erhardt, M., Canaday, J., Gualberto, J.M., and Imbault, P. (2006). The plant-specific ssDNA binding protein OSB1 is involved in the stoichiometric transmission of mitochondrial DNA in Arabidopsis. Plant Cell **18:** 3548–3563.

Zampini, É., Lepage, É., Tremblay-Belzile, S., Truche, S., and Brisson, N. (2015). Organelle DNA rearrangement mapping reveals U-turn-like inversions as a major source of genomic instability in Arabidopsis and humans. Genome Res. **25:** 645–654.

Zhang, J., Mahdi, A.A., Briggs, G.S., and Lloyd, R.G. (2010). Promoting and avoiding recombination: contrasting activities of the *Escherichia coli* RuvABC Holliday junction resolvase and RecG DNA translocase. Genetics **185:** 23–37.